5 Vortex motion

5.1. Kelvin's circulation theorem

THEOREM. *Let an inviscid, incompressible fluid of constant density be in motion in the presence of a conservative body force* $\boldsymbol{g} = -\nabla\chi$ *per unit mass. Let* $C(t)$ *denote a closed circuit that consists of the same fluid particles as time proceeds (Fig. 5.1). Then the circulation*

$$\Gamma = \int_{C(t)} \boldsymbol{u} \cdot \mathrm{d}\boldsymbol{x} \tag{5.1}$$

round $C(t)$ *is independent of time.*

Proof. We appeal to the following lemma:

$$\frac{\mathrm{d}}{\mathrm{d}t}\int_{C(t)} \boldsymbol{u} \cdot \mathrm{d}\boldsymbol{x} = \int_{C(t)} \frac{\mathrm{D}\boldsymbol{u}}{\mathrm{D}t} \cdot \mathrm{d}\boldsymbol{x} \tag{5.2}$$

(Exercise 5.2). Then, by Euler's equation (1.12),

$$\frac{\mathrm{d}\Gamma}{\mathrm{d}t} = -\int_{C(t)} \nabla\left(\frac{p}{\rho} + \chi\right) \cdot \mathrm{d}\boldsymbol{x} = -\left[\frac{p}{\rho} + \chi\right]_C,$$

where the last term denotes the change in $p/\rho + \chi$ on going once round C (see eqn (A.12)). But this change is zero, as p, ρ, and χ are all single-valued functions of position. This proves the theorem.

Notes on the theorem

(a) C denotes a 'dyed' circuit, composed of the same fluid particles as time proceeds; the result is not true in general if C is a closed curve fixed in space.

(b) The conditions of incompressibility and constant density are not essential: Kelvin established his result subject to weaker restrictions (Exercise 5.4).

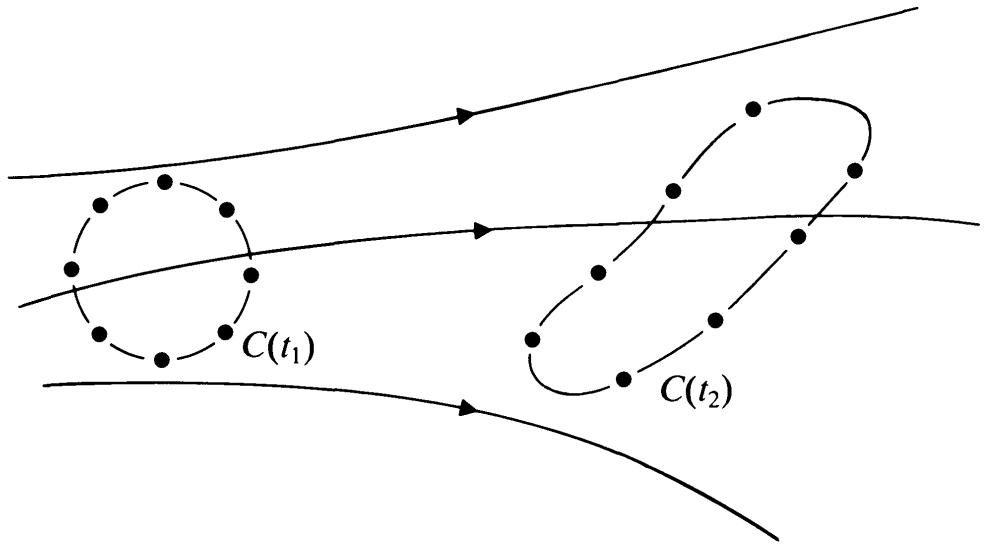

Fig. 5.1. Definition sketch for Kelvin's theorem, showing eight fluid particles along a 'dyed' circuit C at time t_1, and their positions at time t_2.

(c) The theorem does not require the fluid region to be simply connected, i.e. it does not require the dyed circuit C to be spannable by a surface S lying wholly in the fluid.

(d) The inviscid equations of motion enter the proof only in helping to evaluate a line integral round C, so if viscous forces happened to be important elsewhere in the flow, i.e. off the curve C, this would not affect the conclusion that Γ remains constant round C.

The generation of lift on an aerofoil

We mentioned in §1.1 how the shedding of a starting vortex is essential to the generation of lift on an aerofoil, and we now investigate why this should be so.

Consider the situation at a time t after the start. Vorticity and viscous forces will be confined to (i) a thin boundary layer on the aerofoil, (ii) a thin wake, and (iii) the rolled-up 'core' of the starting vortex, as indicated by the shading in Fig. 5.2. Consider now a dyed circuit abcda which is large enough to have been clear of all these regions since the start of the motion. As the original state was one of rest the circulation round that circuit was originally zero. By Kelvin's circulation theorem, then, the circulation round that circuit will still be zero at time t (see especially note (d) above). Thus if we sketch in a line aec—an

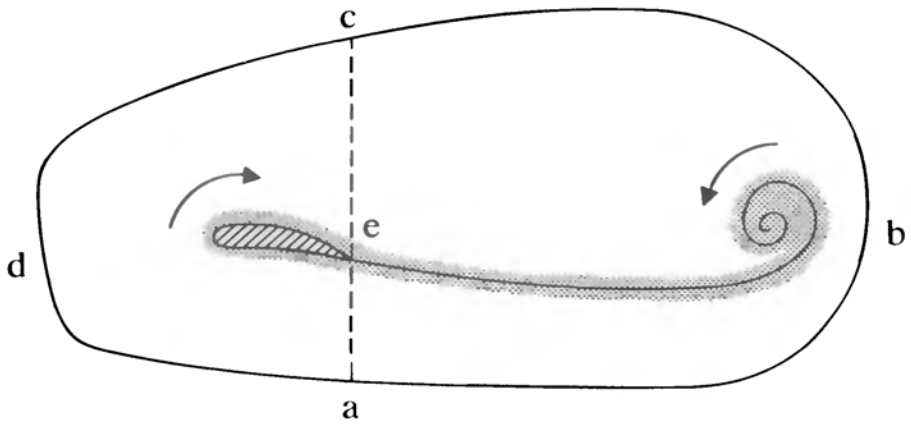

Fig. 5.2. The generation of circulation by means of vortex shedding.

instantaneous line in space at time t such that the curve aecda encloses the aerofoil but not the wake or the starting vortex—then the circulation round aecda must be equal and opposite to that round abcea.

What happens, then, as the aerofoil starts to move, is that positive vorticity is shed in the form of a starting vortex. By Stokes's theorem,

$$\int_S \boldsymbol{\omega} \cdot \boldsymbol{n}\, \mathrm{d}S = \int_C \boldsymbol{u} \cdot \mathrm{d}\boldsymbol{x},$$

this gives a positive circulation round abcea. This in turn implies, by the preceding argument, a negative circulation round aecda, and this circulation is very evident in some classic photographs taken by Prandtl and Tietjens (see, e.g., Batchelor 1967, Plate 13). The vortex shedding continues until the circulation round the aerofoil is sufficient to make the main, irrotational flow smooth at the trailing edge, as in Fig. 1.10(b), at which stage no further net vorticity is shed into the wake from the boundary layers on the upper and lower surfaces of the aerofoil. Thereafter the aerofoil retains its final 'Kutta–Joukowski' value of the circulation.

A novel mechanism of lift generation for hovering insects

An exotic variation on the above theme was discovered by Weis-Fogh (1973, 1975) in the hovering motions of the tiny chalcid wasp *Encarsia formosa* (wing chord ~0.2 mm). This insect claps its wings together, then flings them open about a

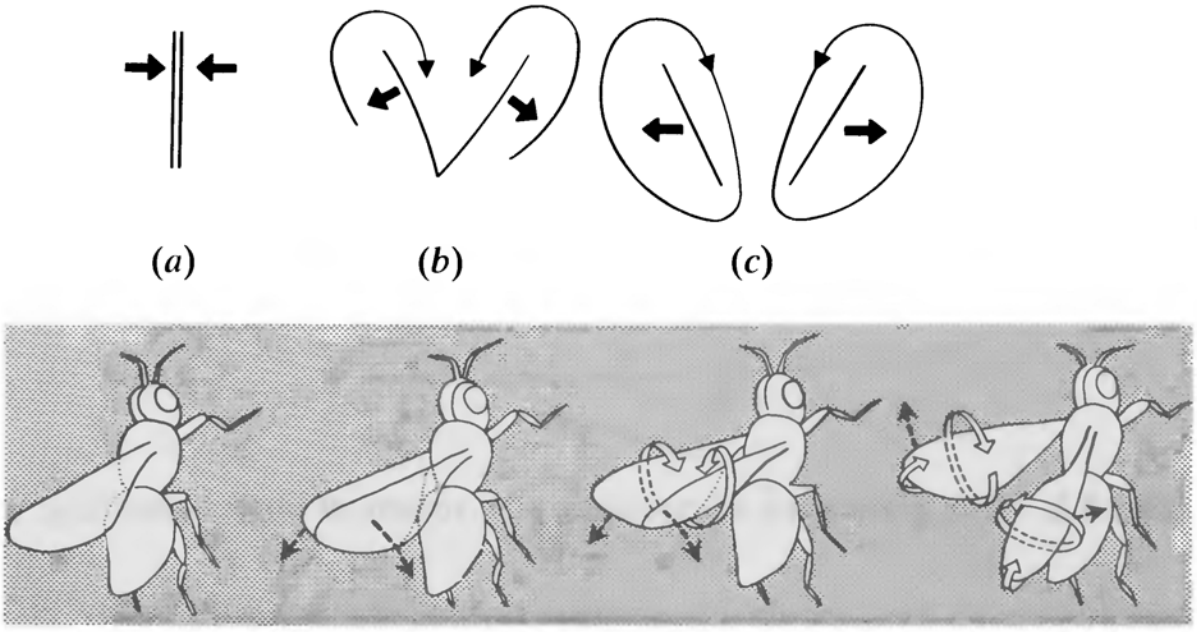

Fig. 5.3. The Weis-Fogh mechanism of lift generation. The first three sketches give a 2-D model of (*a*) the 'clap', (*b*) the 'fling', and (*c*) the parting of the wings. The remaining sketches (after Dalton 1977) show the mechanism in practice, and the final sketch indicates also the flow associated with the vortex (not shown) that extends, in a circular arc, between the wing tips (cf. Fig. 1.12).

horizontal line of contact, so that air has to rush in to fill the gap (Fig. 5.3(*b*)). Then it moves its wings apart, by which time each one has acquired during the 'fling' movement a circulation of the correct sign to give lift in the subsequent motion.

In practice, viscous effects are important, especially in causing large leading-edge separation vortices (see the excellent photographs in Spedding and Maxworthy 1986). Nevertheless, one remarkable feature of this novel lift generation mechanism is that it could work, in principle, in a strictly inviscid fluid (Lighthill 1973). In this sense it differs markedly from the conventional method for lift generation which we have just discussed, for that relies in an essential way on viscous effects for boundary layer formation, separation at the trailing edge, and consequent vortex shedding. In the Weis-Fogh mechanism the circulation round one wing essentially acts as the starting vortex for the other.

At first sight, perhaps, Kelvin's circulation theorem does not permit the situation in Fig. 5.3(*c*) for a strictly inviscid fluid: if one views the circuits there as dyed circuits then the circulations round them must have remained constant. Yet one cannot claim that those circulations are zero, even if the fluid were wholly at

rest at stage (a), for neither dyed circuit at stage (c) was a *closed* circuit at stage (b), an unusual circumstance that arises only because the topology of the fluid domain has changed in the meantime.

The word 'meantime' gives, in fact, rather too leisurely an impression; *Encarsia formosa* goes through the sequence in Fig. 5.3 roughly 400 times a second.

5.2. The persistence of irrotational flow

Let an inviscid, incompressible fluid of constant density move in the presence of a conservative body force. Then if a portion of the fluid is initially in irrotational motion, that portion will always be in irrotational motion.

To prove this *Cauchy–Lagrange theorem* suppose that the vorticity $\boldsymbol{\omega} = \nabla \wedge \boldsymbol{u}$ were *not* identically zero throughout that portion of fluid at a later time. By virtue of Stokes's theorem:

$$\int_C \boldsymbol{u} \cdot \mathrm{d}\boldsymbol{x} = \int_S \boldsymbol{\omega} \cdot \boldsymbol{n} \, \mathrm{d}S,$$

and it would then be possible to select some small closed dyed circuit around which the circulation would be non-zero. But this would violate Kelvin's circulation theorem, because the circulation round such a circuit must initially have been zero, on account of Stokes's theorem and the fact that $\boldsymbol{\omega}$ was initially zero. Our initial assumption must therefore be false. This completes the proof.

For 2-D flows the result is obvious from the vorticity equation (1.27); if ω is zero for a portion of the fluid at $t = 0$ then, according to eqn (1.27), ω remains zero for each fluid element constituting that portion for all time t. But in three dimensions the result is not obvious from eqn (1.25), and it is here that the theorem comes into its own. (Although it is of course quite evident that if $\boldsymbol{\omega}$ is everywhere zero at $t = 0$ then $\boldsymbol{\omega} = 0$ everywhere for all t is *one* solution of eqn (1.25).)

Irrotational flows are important, then, even in three dimensions. The velocity field can then be written as

$$\boldsymbol{u} = \nabla \phi, \tag{5.3}$$

and ϕ will be a single-valued function of position when the flow

region is simply connected (see §4.2). [In other circumstances—as, for example, with the irrotational part of the flow due to a vortex ring (Fig. 5.7(*b*))—ϕ may be multivalued.] As the fluid is incompressible, $\nabla \cdot \boldsymbol{u} = 0$, so ϕ satisfies *Laplace's equation*

$$\nabla^2 \phi = 0. \tag{5.4}$$

The general theory of irrotational flow is a classical and important part of fluid dynamics, and we explore something of it in Exercises 5.23–5.29. We should emphasize, however, that much of the present chapter is concerned with fluid motions in which the vorticity is *not* zero, in which case there is no such thing as a velocity potential ϕ and $\boldsymbol{u}$ *cannot* be written in the form (5.3).

5.3. The Helmholtz vortex theorems

A *vortex line* is, at any particular time t, a curve which has the same direction as the vorticity vector

$$\boldsymbol{\omega} = \nabla \wedge \boldsymbol{u} \tag{5.5}$$

at each point. Mathematically, then, a vortex line $x = x(s)$, $y = y(s)$, $z = z(s)$, is obtained by solving

$$\frac{\mathrm{d}x/\mathrm{d}s}{\omega_x} = \frac{\mathrm{d}y/\mathrm{d}s}{\omega_y} = \frac{\mathrm{d}z/\mathrm{d}s}{\omega_z}$$

at a particular time t.

The vortex lines which pass through some simple closed curve in space are said to form the boundary of a *vortex tube* (Fig. 5.4(*a*)).

Suppose now that we have an *inviscid, incompressible fluid of constant density moving in the presence of a conservative body force* (so that Kelvin's circulation theorem applies). Then

(1) *The fluid elements that lie on a vortex line at some instant continue to lie on a vortex line, i.e. vortex lines 'move with the fluid'.*

An immediate consequence of this is that vortex tubes move with the fluid in a like manner.

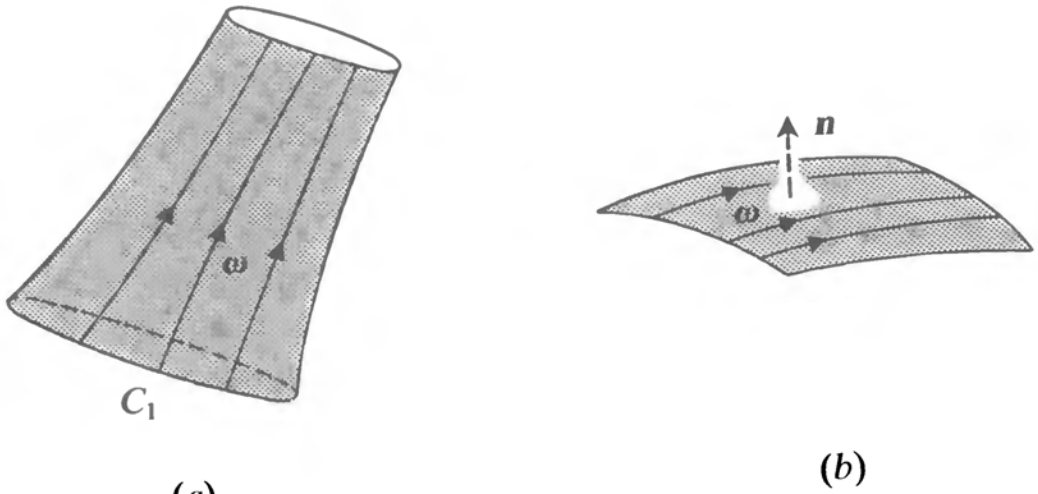

(*a*) (*b*)

Fig. 5.4. (*a*) A vortex tube. (*b*) A vortex surface.

(2) *The quantity*

$$\Gamma = \int_S \boldsymbol{\omega} \cdot \boldsymbol{n} \, \mathrm{d}S \tag{5.6}$$

is the same for all cross-sections S of a vortex tube. Furthermore, Γ is independent of time.

The quantity Γ is therefore a conserved property of the tube as a whole, called the *strength* of the tube.

Proof of (1). We first define a *vortex surface* as a surface such that $\boldsymbol{\omega}$ is tangent to the surface at every point (Fig. 5.4(b)). The proof proceeds by viewing the vortex line, in its initial configuration, as the intersection of two vortex surfaces. Mark the particles which occupy one of the vortex surfaces, at $t = 0$, with dye. Consider a closed circuit C made up of a particular set of dyed particles and spanned by a portion S_* of the vortex surface. At $t = 0$ the circulation round C is zero, for by Stokes's theorem

$$\int_C \boldsymbol{u} \cdot \mathrm{d}\boldsymbol{x} = \int_{S_*} \boldsymbol{\omega} \cdot \boldsymbol{n} \, \mathrm{d}S,$$

and $\boldsymbol{\omega} \cdot \boldsymbol{n}$ is zero on S_*. Now, as time proceeds the dyed sheet of fluid will deform, but the circulation round C will remain zero, by Kelvin's circulation theorem. This being so for all circuits such as C it follows, by using Stokes's theorem again, that $\boldsymbol{\omega} \cdot \boldsymbol{n}$ will remain zero at all points of the dyed sheet of fluid. That sheet therefore remains a vortex surface as time proceeds. The proof is

completed by noting that the intersection of two such dyed sheets therefore remains the intersection of two vortex surfaces, i.e. it remains a vortex line.

Proof of (2). The statement that Γ is independent of the cross-section S has nothing to do with the equations of motion, but is simply a consequence of the fact that the vorticity $\boldsymbol{\omega} = \nabla \wedge \boldsymbol{u}$ is divergence-free (Exercise 5.5). The statement that Γ is independent of time follows on considering a circuit, such as C_1 in Fig. 5.4(*a*), composed of fluid particles which lie on the wall of the vortex tube and encircle it. By Stokes's theorem, Γ is the circulation round C_1, and by Kelvin's circulation theorem this remains constant as time proceeds.

It is instructive to consider the particular case of a *thin* vortex tube in which $\boldsymbol{\omega}$ is virtually constant across any particular cross-section. In that case Γ is essentially just the product $\omega\, \delta S$, where δS is the normal cross-section of the tube. But δS is also the normal cross-section of the fluid continually occupying the tube, and as the fluid must conserve its volume δS will vary inversely with the length l of a small section of the tube. Thus the vorticity ω varies in proportion to l; stretching of vortex tubes by the fluid motion intensifies the local vorticity.

In a tornado, for example, the strong thermal updraughts into the thunderclouds overhead produce intense stretching of vortex tubes, and hence the potentially devastating rotary motions observed. The funnel cloud serves, in fact, as a direct marker of the vortex tube, rather than the air occupying it, because it essentially marks regions of very low pressure (where the air rapidly expands and condenses), and these in turn are located in the core of the vortex, where all the vorticity is concentrated (see Exercise 1.3). Thus when the thunderclouds move on, and the funnel cloud tips over in the manner of Fig. 5.5, we have a vivid illustration of Helmholtz's first vortex theorem at work.

In contrast, it is the shortening of vortex tubes that is responsible for the gradual 'spin-down' of a stirred cup of tea (Fig. 5.6). The main body of the fluid is essentially inviscid and in rapid rotation, the centrifugal force being (almost) balanced by a radially inward pressure gradient. This pressure gradient also imposes itself throughout the thin viscous boundary layer on the

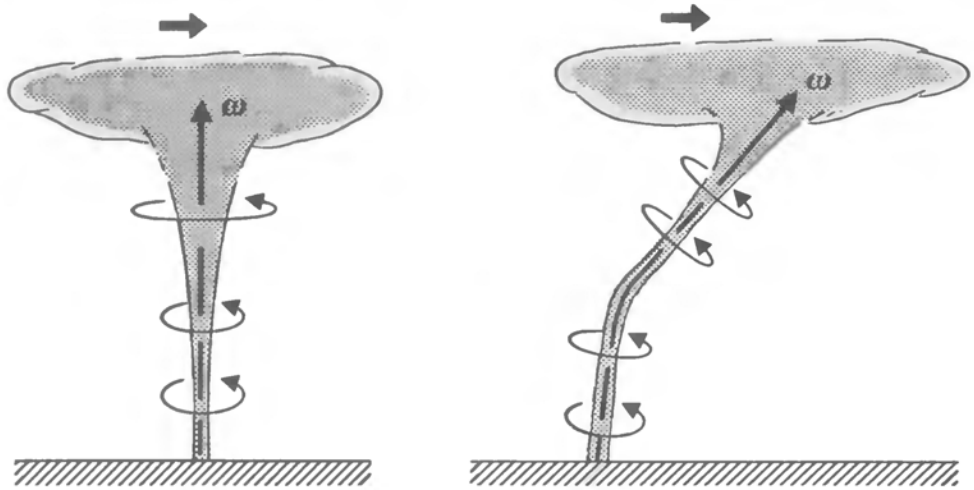

Fig. 5.5. The deformation of a tornado as the thunderclouds move overhead.

bottom of the cup, where it is stronger than required, for the fluid in the boundary layer rotates much less rapidly. That fluid therefore spirals inward (as evinced by the way in which tea leaves on the bottom of the cup congregate in the middle), and eventually turns up and out of the boundary layer, as in Fig. 5.6. In this way vortex tubes in the main body of the fluid become shorter and expand in cross-section, so that the vorticity decreases with time. It is by this subtle mixture of inviscid and viscous dynamics that the apparently innocuous spin-down of a stirred cup of tea is achieved (see §8.5).

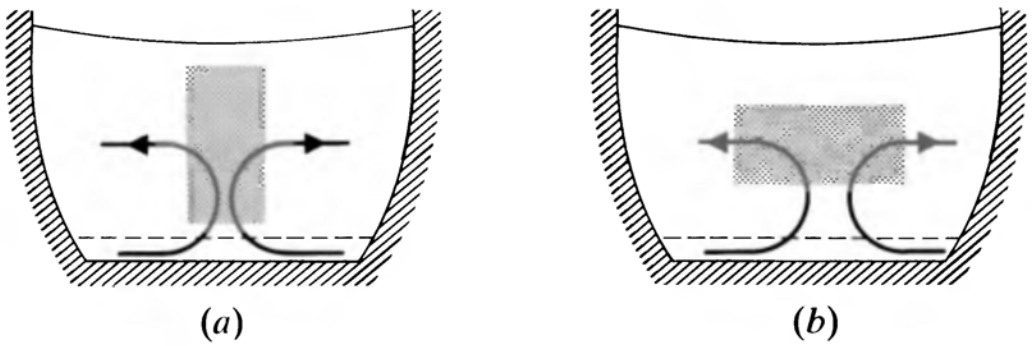

Fig. 5.6. The secondary circulation in a stirred cup of tea is driven by the bottom boundary layer (beneath the dotted line) and turns a tall, thin column of 'dyed' fluid into a short, fat one, so decreasing its angular velocity.

The Helmholtz vortex theorems and the vorticity equation

The vortex theorems above were first given by Helmholtz in 1858, but Kelvin did not obtain and publish his circulation theorem until 1867. It goes without saying, then, that Helmholtz took a different route; he appealed directly to the vorticity equation (1.25):

$$\frac{\mathrm{D}\boldsymbol{\omega}}{\mathrm{D}t} = (\boldsymbol{\omega} \cdot \nabla)\boldsymbol{u}. \tag{5.7}$$

We will not give his actual argument here,† but consider instead the relationship between eqn (5.7) and the vortex theorems in some simple specific cases.

It is possible, for instance, to see by inspection of eqn (5.7) how stretching the fluid that lies along a vortex line leads to an intensification of the local vorticity field. Suppose, for example, that the vortex lines are almost in the z-direction, as in Fig. 5.5(a), so that $\boldsymbol{\omega} \doteqdot \omega \boldsymbol{k}$ and

$$\frac{\mathrm{D}\boldsymbol{\omega}}{\mathrm{D}t} \doteqdot \omega \frac{\partial \boldsymbol{u}}{\partial z}. \tag{5.8}$$

The z-component of this equation gives

$$\frac{\mathrm{D}\omega}{\mathrm{D}t} \doteqdot \omega \frac{\partial w}{\partial z},$$

and the vorticity of a particular fluid element therefore increases with time if $\partial w/\partial z > 0$, i.e. if the instantaneous vertical velocity increases with z. Such is the case, of course, if fluid elements are being stretched in the vertical direction, whereas if they were being carried up or down without any vertical stretching or squashing, w would be independent of z.

A particularly simple case is that of 2-D flow. Vortex tubes are aligned with the z-axis, and $w = 0$. There is no stretching of vortex tubes, and

$$\frac{\mathrm{D}\omega}{\mathrm{D}t} = 0, \tag{5.9}$$

† It in fact contains a flaw, which may however be corrected (see, e.g. Lamb 1932, p. 206; Rosenhead 1963, pp. 122–123).

so that the vorticity ω of any particular fluid element is conserved.

A more revealing case in the present context is that of *axisymmetric* flow:

$$\boldsymbol{u} = u_R(R, z, t)\boldsymbol{e}_R + u_z(R, z, t)\boldsymbol{e}_z, \tag{5.10}$$

where (R, ϕ, z) denote cylindrical polar coordinates.† The velocity components are then independent of ϕ, the streamlines all lie in planes $\phi =$ constant, and the vorticity is $\boldsymbol{\omega} = \omega \boldsymbol{e}_\phi$, where

$$\omega = \frac{\partial u_R}{\partial z} - \frac{\partial u_z}{\partial R}. \tag{5.11}$$

In axisymmetric flow the vortex tubes are therefore ring-shaped, around the symmetry axis. According to the first vortex theorem they move with the fluid. In doing so they will, in general, expand and contract about the symmetry axis, and thus change in length. As the fluid is incompressible the cross-sectional area δS of a thin tube will be in inverse proportion to the length $2\pi R$ of the tube. But the second vortex theorem implies that $\omega\, \delta S$ will be a constant, so we conclude that ω will be proportional to the length of the tube $2\pi R$. We leave it as an instructive exercise (Exercise 5.7) to show that in the case of axisymmetric flow the vorticity equation (5.7) reduces to

$$\frac{\mathrm{D}}{\mathrm{D}t}\left(\frac{\omega}{R}\right) = 0, \tag{5.12}$$

which expresses just this result, that the vorticity of any particular fluid element changes in proportion to R as time proceeds.

When, in axisymmetric flow, an isolated vortex tube is surrounded by irrotational motion, we speak of it as a *vortex ring*. The familiar 'smoke-ring' is perhaps the most common example, and provides a vivid illustration of the Helmholtz vortex theorems, though the vortex core typically occupies only a fraction of the smoke ring as a whole (see Fig. 5.7).

---

† This is not our usual notation, as we are shortly to use spherical polar coordinates (r, θ, ϕ) for axisymmetric flow. It seemed best not to have the same symbol meaning two different things in the space of a few pages. Thus ϕ has the same meaning in the two cases, and $R = r \sin\theta$.

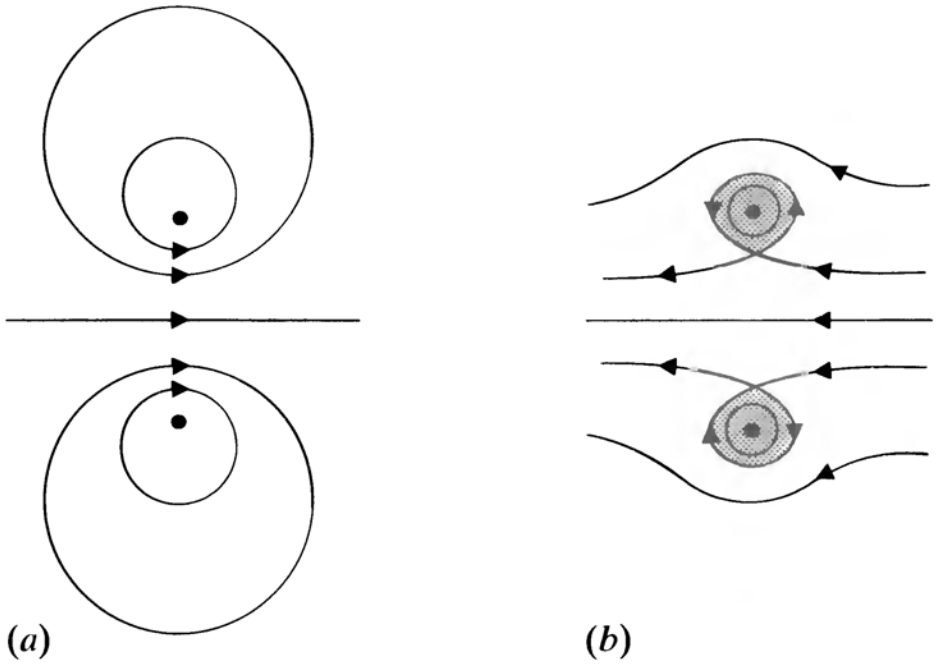

Fig. 5.7. Flow due to a vortex ring (*a*) relative to a fixed frame and (*b*) relative to a frame moving with the vortex core. Shading denotes smoke, in the case of a smoke ring, while the vortex core is indicated by the black dots.

5.4. Vortex rings

We showed in §5.1 how Kelvin's circulation theorem plays a key part in the mechanism by which an aircraft obtains lift at take-off. While this is one of the theorem's most elegant and significant applications, it is not of course what Kelvin had in mind in 1867. What he did have in mind is quite extraordinary, but clear enough from the following:

Jan. 22, 1867.

MY DEAR HELMHOLTZ—I have allowed too long a time to pass without thanking you for your kind letter .... Just now, ... *Wirbelbewegungen* have displaced everything else, since a few days ago Tait showed me in Edinburgh a magnificent way of producing them. Take one side (or the lid) off a box (any old packing-box will serve) and cut a large hole in the opposite side. Stop the open side loosely with a piece of cloth, and strike the middle of the cloth with your hand. If you leave anything smoking in the box, you will see a magnificent ring shot out by every blow. A piece of burning phosphorus gives very good smoke for the purpose; but I think nitric acid with pieces of zinc thrown into it, in the bottom of the box, and cloth wet with ammonia, or a large open dish of ammonia beside it, will answer better. The nitrite of ammonia makes fine white clouds in the air, which, I think, will be less

pungent and disagreeable than the smoke from the phosphorus. We sometimes can make one ring shoot through another, illustrating perfectly your description; when one ring passes near another, each is much disturbed, and is seen to be in a state of violent vibration for a few seconds, till it settles again into its circular form. The accuracy of the circular form of the whole ring, and the fineness and roundness of the section, are beautifully seen. If you try it, you will easily make rings of a foot in diameter and an inch or so in section, and be able to follow them and see the constituent rotary motion. The vibrations make a beautiful subject for mathematical work. The solution for the longitudinal vibration of a straight vortex column comes out easily enough. The absolute permanence of the rotation, and the unchangeable relation you have proved between it and the portion of the fluid once acquiring such motion in a perfect fluid, shows that if there is a perfect fluid all through space, constituting the substance of all matter, a vortex-ring would be as permanent as the solid hard atoms assumed by Lucretius and his followers (and predecessors) to account for the permanent properties of bodies (as gold, lead, etc.) and the differences of their characters. Thus, if two vortex-rings were once created in a perfect fluid, passing through one another like links of a chain, they never could come into collision, or break one another, they would form an indestructible atom; every variety of combinations might exist. Thus a long chain of vortex-rings, or three rings, each running through each of the other, would give each very characteristic reactions upon other such kinetic atoms.

This atomic theory,† 40 years ahead of that of Niels Bohr, was no speculative sideline to Kelvin's hydrodynamic researches at the time; it was the main impetus behind them, and in the opening sentence of his 1867 paper he more or less says as much.

One hundred and twenty years later, vortex rings still exercise a certain fascination, although more modest and less dangerous ways of producing them are perhaps to be recommended. All that is needed is some arrangement for discharging smoke through a circular hole in a plane rigid boundary, where separation of the boundary layer can take place and be followed by the rolling up of the consequent vortex sheet (Fig. 5.9). Any simple apparatus which achieves this will suffice; I employ a syringe of the kind commonly used to squeeze icing on to cakes.

† Atiyah (1988) observes that one particular notion in this theory—that of using topology as a source of stability—may be said to have surfaced again in modern physics, albeit in a different guise.

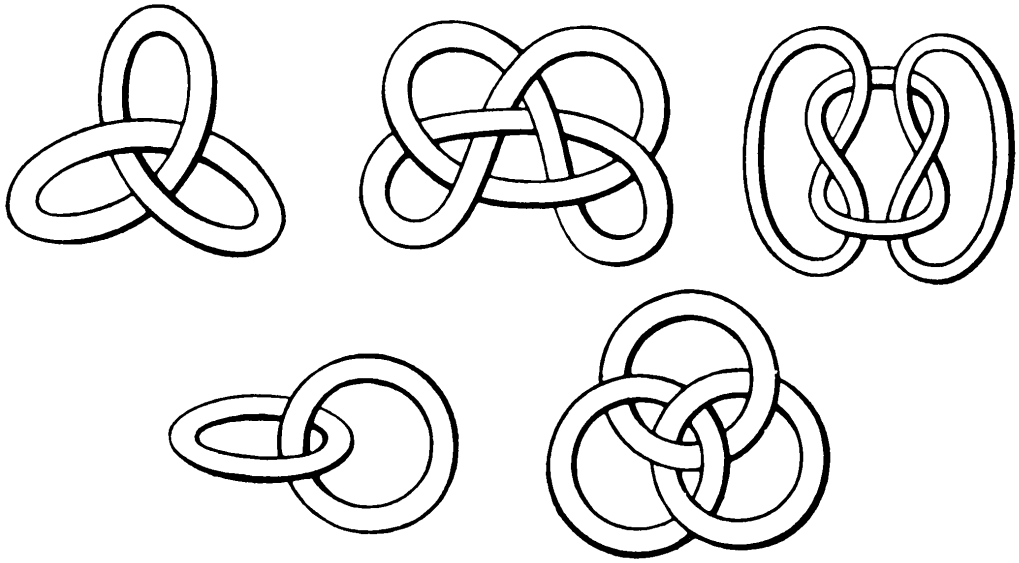

Fig. 5.8. Kelvin's sketches of knotted and linked vortex rings, the basis for his 'vortex atom' theory of matter.

A satisfactory procedure, having detached the nozzle itself, is as follows. Push the piston fully in, then puff cigar smoke through the circular hole while rapidly withdrawing the piston, so that the smoke is sucked into the syringe. As soon as the piston is fully withdrawn, put a hand over the hole to keep the smoke in. Allow a few moments for the motions inside to die down, and then generate vortex rings by holding the cylinder horizontally and giving the piston short, sharp taps. Each ring should travel a foot or so while maintaining its form, provided that the surrounding air is fairly still.

Helmholtz considered vortex rings in his 1858 paper, and after deducing that rings of smaller radius travel faster, went on:

> We can ... see how two ring-formed vortex filaments having the same axis would mutually affect each other, since each, in addition to its proper motion, has that of its elements of fluid as produced by the other ...

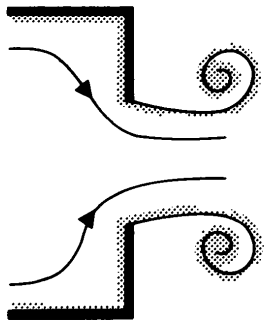

Fig. 5.9. Generation of a vortex ring by the discharge of fluid through a circular hole.

If they have equal radii and equal and opposite angular velocities, they will approach each other and widen one another; so that finally, when they are very near each other, their velocity of approach becomes smaller and smaller, and their rate of widening faster and faster. If they are perfectly symmetrical, the velocity of fluid elements midway between them parallel to the axis is zero. Here, then, we might imagine a rigid plane to be inserted, which would not disturb the motion, and so obtain the case of a vortex-ring which encounters a fixed plane.

The last sentence is, of course, an interesting example of the method of images, while in saying earlier 'they will approach each other *and widen one another*' Helmholtz is applying his first vortex theorem.

He considers, too, the case when the vortex rings are travelling in the same direction. On the same basis he deduces:

> . . . the foremost widens and travels more slowly, the pursuer shrinks and travels faster, till finally, if their velocities are not too different, it overtakes the first and penetrates it. Then the same game goes on in the opposite order, so that the rings pass through each other alternately.

Good photographs of this 'leap-frogging' phenomenon may be found in Yamada and Matsui (1978), in Oshima (1978) and on p. 46 of van Dyke (1982). In practice, of course, viscous effects act to stop such leap-frogging from continuing indefinitely; indeed they have profound effects, more generally, on the behaviour of real vortex rings (Maxworthy 1972).

Kelvin was of course well aware that real vortex rings do not, on account of viscous effects, wholly retain their identity in the manner indicated by Helmholtz's vortex theorems. One nevertheless wonders, given his hopes for the theory of vortex atoms, what he would have made of an experiment by Oshima and Asaka (1975) in which a red vortex ring and a yellow vortex ring (in water) collide at a certain angle. The rings merge, then break up again into two separate rings, each half yellow and half red. The way in which they do this is indicated in Fig. 5.10. In (*a*) the vortex rings are coming towards us, but they are also approaching one another. In (*b*) they collide, and after a distortion (*c*) of the resulting (single) vortex ring two separate rings are formed (*d*). These come towards us but move apart in a plane at right angles to the plane of approach. Oshima and Asaka provide excellent photographs of this collision process, and further photographs and analysis may be found in Fohl and Turner (1975).

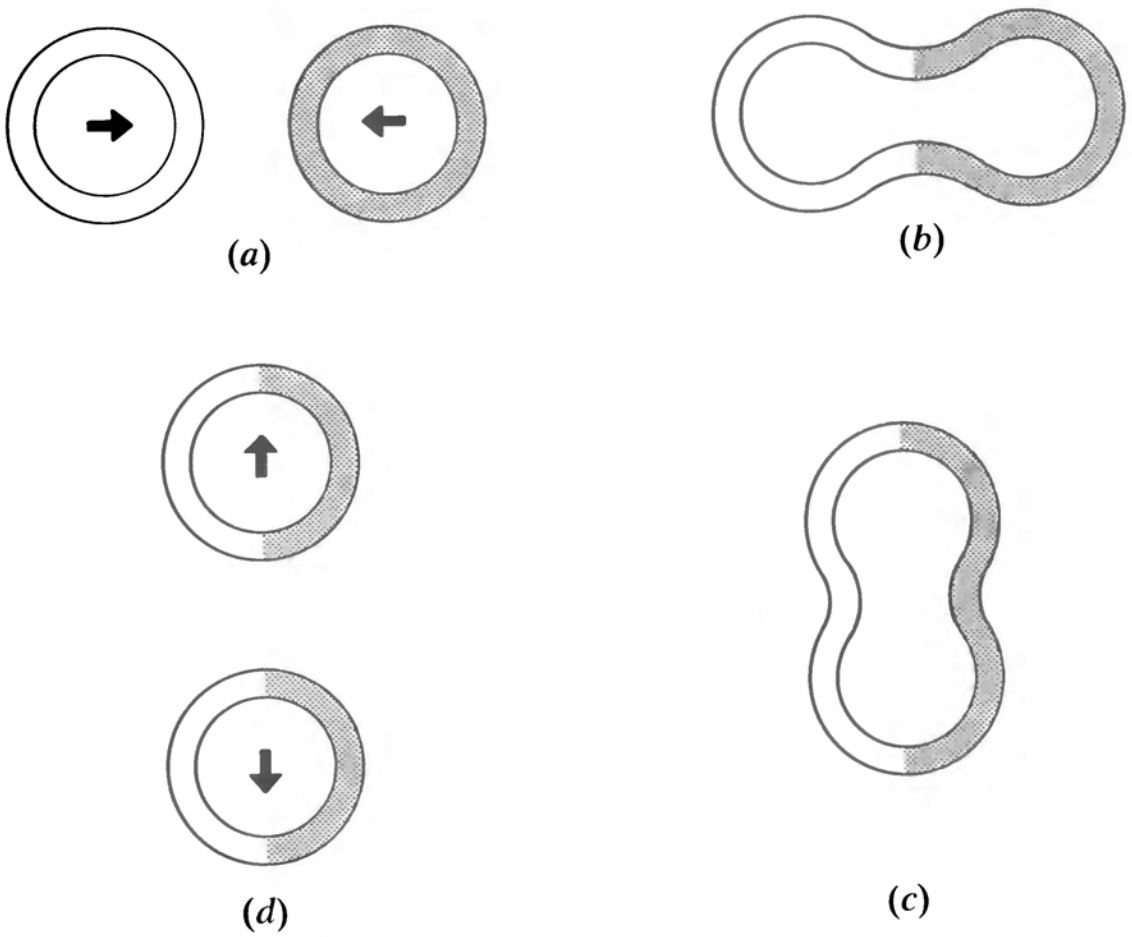

Fig. 5.10. The collision of two viscous vortex rings.

Even within the framework of strictly inviscid theory there are subtle aspects of vortex rings which have taken a long time to emerge. Kelvin himself expressed the view that 'the known phenomena of . . . smoke rings . . . convinces . . . us . . . that the steady configuration . . . is stable', and J. J. Thomson purported to demonstrate as much in his 1883 essay, *A treatise on vortex motion*. But Widnall and Tsai (1977) have carried out a more accurate calculation, and have shown that a vortex ring is in fact unstable, even according to ideal flow theory. The instability takes the form of bending waves around the perimeter, and these grow in amplitude as time proceeds (Fig. 5.11).

5.5. Axisymmetric flow

The uniform motion of a vortex ring—let alone its instability—presents theoretical difficulties, but there is one particular circumstance in which it is quite easy to calculate the self-induced motion of an isolated, axisymmetric patch of vorticity. Before doing this we introduce one or two concepts that are of more general value for axisymmetric flow.

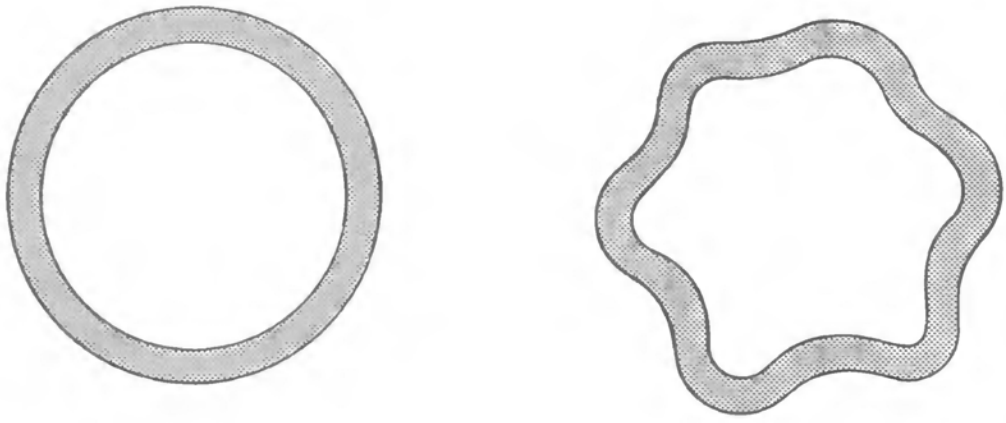

(*a*) $t=t_1$ (*b*) $t=t_2>t_1$

Fig. 5.11. The instability of a vortex ring.

The Stokes stream function

For incompressible flow in two dimensions the stream function representation (4.8) ensures that $\nabla \cdot \boldsymbol{u} = 0$ is automatically satisfied. It is natural to enquire, then, whether for axisymmetric incompressible flow a representation of the form $\boldsymbol{u} = \nabla \wedge (\psi' \boldsymbol{e}_\phi)$ exists, ψ' being a function of R, z, and t only.

This is indeed the case, but a minor inconvenience is that ψ' turns out to be not constant along streamlines, but inversely proportional to R. We therefore write instead

$$\boldsymbol{u} = \nabla \wedge \left(\frac{\Psi}{R} \boldsymbol{e}_\phi \right), \tag{5.13}$$

or, in spherical polars,

$$\boldsymbol{u} = \nabla \wedge \left(\frac{\Psi}{r \sin \theta} \boldsymbol{e}_\phi \right), \tag{5.14}$$

whence

$$u_r = \frac{1}{r^2 \sin \theta} \frac{\partial \Psi}{\partial \theta}, \qquad u_\theta = -\frac{1}{r \sin \theta} \frac{\partial \Psi}{\partial r}, \tag{5.15}$$

Ψ being a function of r, θ, and t only. We may verify immediately that

$$(\boldsymbol{u} \cdot \nabla)\Psi = u_r \frac{\partial \Psi}{\partial r} + \frac{u_\theta}{r} \frac{\partial \Psi}{\partial \theta} = 0.$$

Thus the *Stokes stream function* Ψ, defined by eqn (5.15), is *constant along streamlines.*

Irrotational flow past a sphere

In steady axisymmetric flow the vorticity equation (5.12) reduces to

$$(\boldsymbol{u}\cdot\nabla)\left(\frac{\omega}{r\sin\theta}\right)=0, \tag{5.16}$$

so that $\omega/r\sin\theta$ is constant along streamlines. Consider, then, uniform inviscid flow past a rigid sphere $r=a$. If there are no closed streamlines in the flow, i.e. if all streamlines originate at infinity, where ω is zero, then ω is zero everywhere in $r>a$, so the flow is irrotational.

Now, the vorticity in axisymmetric flow is $\boldsymbol{\omega}=\omega\boldsymbol{e}_\phi$, where

$$\omega=\frac{1}{r}\frac{\partial}{\partial r}(ru_\theta)-\frac{1}{r}\frac{\partial u_r}{\partial\theta}, \tag{5.17}$$

and this may be expressed in terms of the Stokes stream function as follows:

$$\omega=-\frac{1}{r\sin\theta}\left[\frac{\partial^2\Psi}{\partial r^2}+\frac{\sin\theta}{r^2}\frac{\partial}{\partial\theta}\left(\frac{1}{\sin\theta}\frac{\partial\Psi}{\partial\theta}\right)\right]. \tag{5.18}$$

Thus, for irrotational flow past a sphere, we wish to solve

$$\frac{\partial^2\Psi}{\partial r^2}+\frac{\sin\theta}{r^2}\frac{\partial}{\partial\theta}\left(\frac{1}{\sin\theta}\frac{\partial\Psi}{\partial\theta}\right)=0. \tag{5.19}$$

in $r\geqslant a$, subject to $\Psi=0$ on $r=a$ and

$$u_r\sim U\cos\theta,\quad u_\theta\sim -U\sin\theta\qquad \text{as } r\to\infty,$$

which, on using eqn (5.15), means

$$\Psi\sim\tfrac{1}{2}Ur^2\sin^2\theta\qquad \text{as } r\to\infty. \tag{5.20}$$

This last condition suggests trying a separable solution of the form $\Psi=f(r)\sin^2\theta$, and this is indeed possible if

$$f''-\frac{2f}{r^2}=0,$$

i.e. if

$$f=Ar^2+\frac{B}{r}.$$

The boundary conditions then determine the arbitrary constants A and B, whence

$$\Psi = \tfrac{1}{2}U\left(r^2 - \frac{a^3}{r}\right)\sin^2\theta \qquad \text{in } r \geqslant a. \tag{5.21}$$

The streamlines $\Psi =$ constant are sketched in Fig. 5.12(a). There is, inevitably, a velocity of slip

$$u_\theta = -\frac{1}{r\sin\theta}\frac{\partial\Psi}{\partial r} = -\tfrac{3}{2}U\sin\theta \qquad \text{on } r = a, \tag{5.22}$$

and this implies, by Bernoulli's theorem, a severe adverse pressure gradient over the back of the sphere. In real, high Reynolds number flow past a sphere, no attached boundary layer can cope with this adverse pressure gradient, and separation of the boundary layer leads instead to a large wake (see §§2.1 and 8.6).

Hill's spherical vortex

Let us now suppose instead that the region $r < a$ is also filled with fluid. Remarkably, it is possible to find a closed-streamline inviscid flow in $r < a$ which matches on to eqn (5.21) in the sense that (i) Ψ is zero on $r = a$ and (ii) the tangential component of velocity u_θ matches with eqn (5.22) on $r = a$.

In this closed-streamline region (5.16) tells us only that $\omega/r\sin\theta$ is constant along each streamline; there is no reason to suppose it is the same constant along each one, let alone zero.

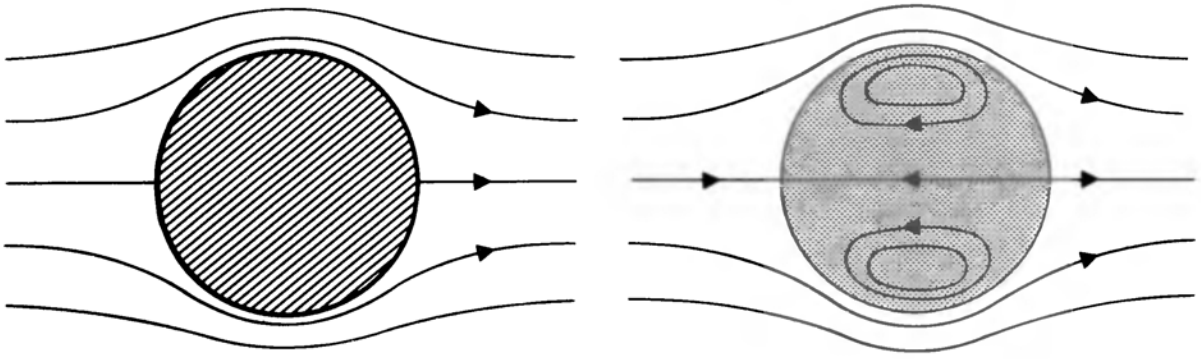

(a) (b)

Fig. 5.12. (a) Irrotational flow past a sphere. (b) Hill's spherical vortex.

The most we can claim, then, is that

$$\frac{\omega}{r\sin\theta} = c(\Psi) \qquad \text{in } r \leqslant a,$$

where the function $c(\Psi)$ is at this stage unknown. Using eqn (5.18) this implies that

$$\frac{\partial^2\Psi}{\partial r^2} + \frac{\sin\theta}{r^2}\frac{\partial}{\partial\theta}\left(\frac{1}{\sin\theta}\frac{\partial\Psi}{\partial\theta}\right) = -c(\Psi)r^2\sin^2\theta \qquad (5.23)$$

is $r \leqslant a$, and $c(\Psi)$ is to be determined as part of the solution (if, indeed, such a solution exists).

Now, in order that u_θ matches with eqn (5.22) on $r = a$ we need

$$\frac{\partial\Psi}{\partial r} = \tfrac{3}{2}Ua\sin^2\theta \qquad \text{on } r = a, \qquad (5.24)$$

and this suggests trying $\Psi = g(r)\sin^2\theta$ in eqn (5.23). The left-hand side is then a function of r times $\sin^2\theta$, and the form of the right-hand side then shows that $c(\Psi)$ will need to be a constant, c, if eqn (5.23) is to reduce to an ordinary differential equation for $g(r)$. The function $g(r)$ then emerges as

$$g(r) = Ar^2 + \frac{B}{r} - \tfrac{1}{10}cr^4.$$

We must choose $B = 0$ to keep $\boldsymbol{u}$ finite at $r = 0$, and A must then be chosen so that $\Psi = 0$ on $r = a$. Finally, eqn (5.24) implies that $c = -15U/2a^2$, so

$$\Psi = -\tfrac{3}{4}Ur^2\left(1 - \frac{r^2}{a^2}\right)\sin^2\theta \qquad \text{in } r \leqslant a. \qquad (5.25)$$

The corresponding streamlines are sketched in Fig. 5.12(b).

The circulation round these streamlines varies from one to the other, of course, because the flow in $r \leqslant a$ has vorticity, but the circulation round the perimeter of a full hemispherical cross-section is, by Stokes's theorem,

$$\Gamma_{\max} = \int_0^\pi \int_0^a \omega r \, \mathrm{d}r \, \mathrm{d}\theta = c\int_0^\pi \int_0^a r^2\sin\theta \, \mathrm{d}r \, \mathrm{d}\theta = -5Ua.$$

Equivalently, a Hill spherical vortex will travel through stationary fluid with uniform speed $\Gamma_{max}/5a$, distinguished from an ordinary smoke ring by the absence of a hole and by the way in which the vorticity is spread throughout the whole of the closed streamline region (cf. Fig. 5.7(*b*)).

5.6. Motion of a vortex pair

We now explore some aspects of 2-D vortex motion. Consider, for instance, the vortex pair of Fig. 5.13(*a*), and suppose that the core of each vortex, where all the vorticity is concentrated, is quite small. The fluid momentarily occupying one of the vortex cores will be swept downwards by the flow due to the other vortex, and by eqn (5.9) that fluid will retain its vorticity, so the vortex itself will be swept downwards. The two vortices therefore move down together, maintaining their relative positions. It is possible to observe this at airports by watching the trailing vortices from the wing-tips of departing aircraft (see Fig. 1.12(*b*)).

To make these ideas more specific we *treat each vortex as a line vortex which moves at the local flow velocity due to everything other than itself.* If the vortices are of strength Γ and $-\Gamma$, distance $2d$ apart, then each will induce a downward flow $\Gamma/4\pi d$ at the

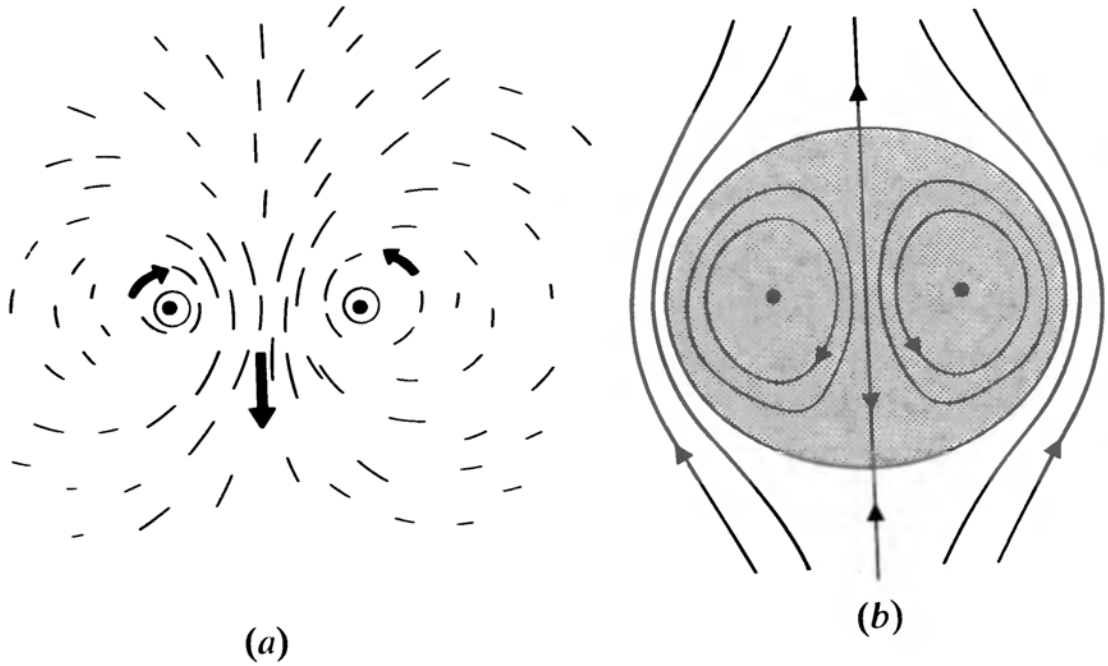

Fig. 5.13. Flow due to a vortex pair relative to (*a*) a fixed frame and (*b*) a frame moving with the vortices.

position momentarily occupied by the other, so the pair itself, and the whole instantaneous streamline pattern, will move downwards at this speed.

We may alternatively view the motion from a frame in which the vortices are fixed. This in turn is equivalent to superimposing a uniform upward flow with speed $\Gamma/4\pi d$, i.e. just that required to hold the vortices at rest. The complex potential for the resulting flow is clearly

$$w = -\frac{\mathrm{i}\Gamma z}{4\pi d} - \frac{\mathrm{i}\Gamma}{2\pi}\log(z-d) + \frac{\mathrm{i}\Gamma}{2\pi}\log(z+d), \tag{5.26}$$

the first term representing the uniform upward flow, and the others representing the flows due to the two vortices. To confirm that the vortex at $z = d$ may indeed remain stationary in this situation we calculate the contribution to $\mathrm{d}w/\mathrm{d}z$ at $z = d$ from everything but the vortex at $z = d$ itself. Thus if (U, V) denotes the translational velocity of the vortex at $z = d$ then

$$\begin{aligned} U - \mathrm{i}V &= \left[\frac{\mathrm{d}}{\mathrm{d}z}\left\{\frac{-\mathrm{i}\Gamma z}{4\pi d} + \frac{\mathrm{i}\Gamma}{2\pi}\log(z+d)\right\}\right]_{z=d} \\ &= \left[\frac{-\mathrm{i}\Gamma}{4\pi d} + \frac{\mathrm{i}\Gamma}{2\pi(z+d)}\right]_{z=d} = 0. \end{aligned} \tag{5.27}$$

The stream function for the flow (5.26) is

$$\begin{aligned} \psi &= -\frac{\Gamma x}{4\pi d} - \frac{\Gamma}{2\pi}\log\left|\frac{z-d}{z+d}\right| \\ &= -\frac{\Gamma}{4\pi}\left[\frac{x}{d} + \log\left\{\frac{(x-d)^2+y^2}{(x+d)^2+y^2}\right\}\right]. \end{aligned}$$

The streamlines are sketched in Fig. 5.13(b). If the fluid in the closed streamline region were dyed, an observer in the original frame would see this dyed fluid moving downward as a coherent entity, without change of shape. This is by no means unexpected, of course, as we are now dealing with a 2-D counterpart to the vortex ring of Fig. 5.7.

5.7. Vortices in flow past a circular cylinder

Let a circular cylinder of radius a be initially at rest in a fluid of kinematic viscosity ν. Suppose that it is suddenly translated with

speed U perpendicular to its axis, and suppose too that the Reynolds number

$$R = \frac{2aU}{\nu} \tag{5.28}$$

is somewhere in the region of 200 or so. With the simple home apparatus of §1.1 this might be achieved, for example, with the refill from a ballpoint pen (radius ~2 mm) and a towing speed U of about 5 cm s^{-1}.

The initial phase: almost irrotational flow

According to inviscid theory the response of the fluid to the motion of the cylinder will be determined by the vorticity equation (5.9):

$$\frac{D\omega}{Dt} = 0,$$

which says that the vorticity of each individual fluid element is conserved. Each has zero vorticity initially, as the fluid is at rest. Each element therefore continues to have zero vorticity and the subsequent flow is irrotational.

Consider now the real, viscous situation. During a very short initial phase, which is over by the time the cylinder has moved a distance comparable to its radius, the flow relative to the cylinder is indeed predominantly irrotational, as in Fig. 4.4(*a*). There is intense vorticity in the rapidly thickening boundary layer on the cylinder, but despite the large adverse pressure gradient at the rear of the cylinder there simply has not yet been time for separation to occur, and the vorticity in the boundary layer has not therefore found its way into the main flow.

During this initial phase irrotational flow theory plays a major role by determining the velocity at the edge of the boundary layer. This is important, for in impulsively started flows of this kind reversed flow in the boundary layer first occurs at the place where the velocity at the edge of the boundary layer decreases most rapidly with distance along the boundary. In the case of a circular cylinder, this place is the rear stagnation point, so this is where reversed flow first occurs (Fig. 5.14(*a*)).

Flow at a later stage: the von Kármán vortex street

Thereafter the flow diverges substantially from that predicted by irrotational flow theory. The two attached eddies behind the cylinder grow in size, as in Fig. 5.14(*b*). At a later time still the flow ceases to be symmetric about the centreline (Fig. 5.14(*c*)) and, even more strangely, it ceases to be steady relative to the cylinder, even though the flow at infinity (relative to the cylinder) is constant. Instead, the flow settles into an unsteady but highly structured form in which vortices are shed alternately from the two sides of the cylinder, so giving the remarkable *von Kármán vortex street* of Fig. 5.14(*d, e*).

Von Kármán's interest in the phenomenon stemmed from about 1911, when he was a graduate assistant in Prandtl's laboratory in Göttingen. He tells of those early days in his *Aerodynamics* (1954):

> . . . Prandtl had a doctoral candidate, Karl Hiemenz, to whom he gave the task of constructing a water channel in which he could observe the separation of the flow behind a cylinder. The object was to check experimentally the separation point calculated by means of the boundary-layer theory. For this purpose, it was first necessary to know the pressure distribution around the cylinder in a steady flow. Much to his surprise, Hiemenz found that the flow in his channel oscillated violently.
>
> When he reported this to Prandtl, the latter told him: 'Obviously your cylinder is not circular.'
>
> However, even after very careful machining of the cylinder, the flow continued to oscillate. Then Hiemenz was told that possibly the channel was not symmetric, and he started to adjust it.
>
> I was not concerned with this problem, but every morning when I came in the laboratory I asked him, 'Herr Hiemenz, is the flow steady now?'
>
> He answered very sadly, 'It always oscillates.'

It must be said that this picture of events is valid for a certain range of Reynolds numbers only. Thus at $R = 2000$ the wake is essentially turbulent, with only traces of the periodic structure of Fig. 5.14(*d, e*). At $R = 30$, on the other hand, the wake develops into two symmetrically disposed vortices which remain attached as time proceeds, much as in Fig. 5.14(b). There are many

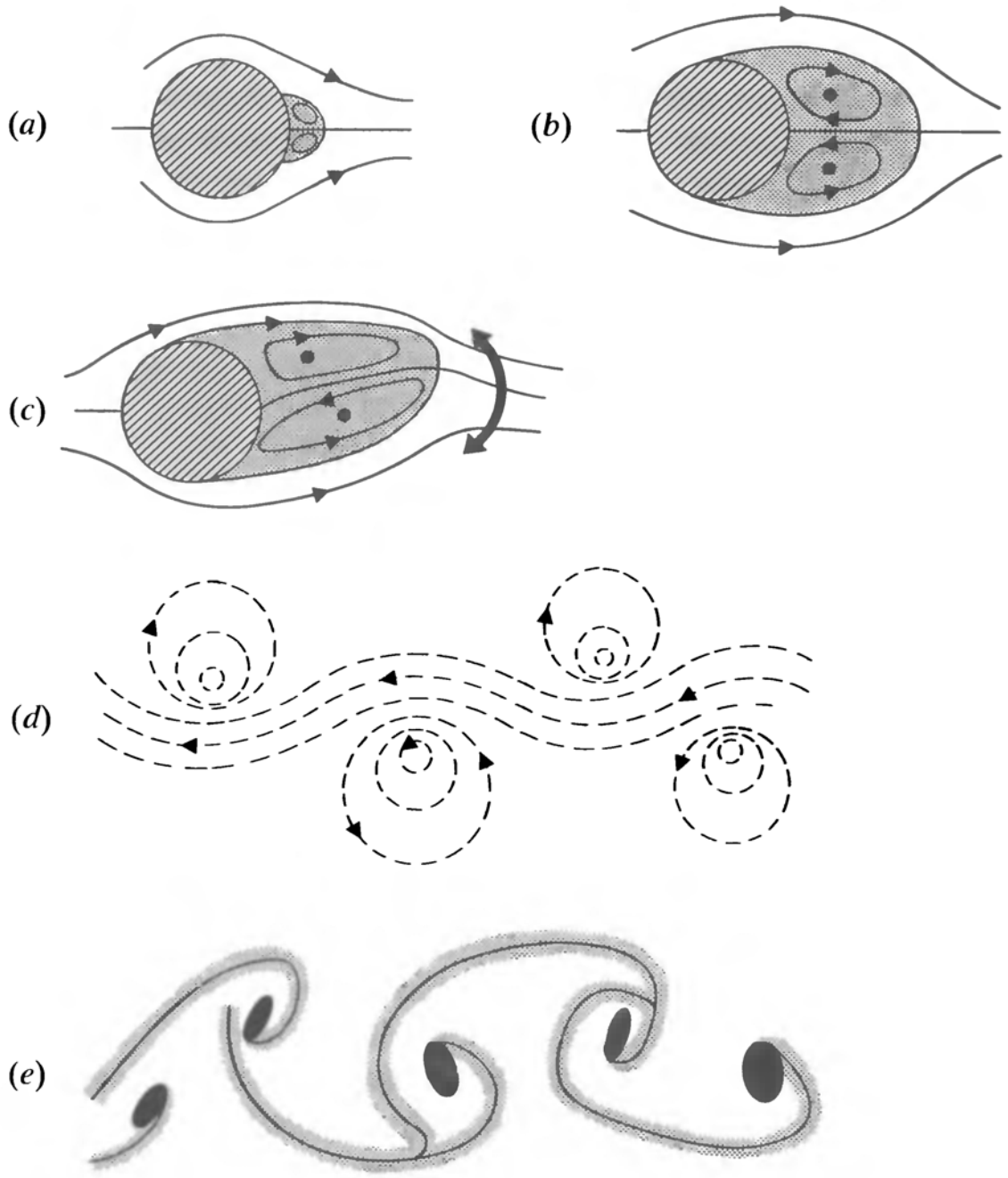

Fig. 5.14. Time-development of flow due to an impulsively moved circular cylinder. (*a*), (*b*), (*c*) Instantaneous streamlines *relative to axes moving with the cylinder* at three fairly early times. (*d*) The instantaneous streamlines, as implied by a streak photograph, *relative to fixed axes,* at a rather later time; the cylinder has moved out of the picture and left behind a trail of von Kármán vortices which follow it by moving to the left at a much slower speed than that of the cylinder. (*e*) At that same later time, typical dye traces, the dye essentially marking those fluid elements which were, at $t = 0$, close to the cylinder boundary; to a fair degree, then, the dye traces also mark regions of strong vorticity.

excellent photographs in the literature of these attached vortices (Coutanceau and Bouard 1977; van Dyke 1982, pp. 28–30), the early evolution of the wake at rather higher Reynolds number (Prandtl and Tietjens 1934, pp. 279–280; Bouard and Coutanceau 1980; van Dyke 1982, pp. 36–37; Perry *et al.* 1982; Loc and Bouard 1985), the subsequent von Kármán vortex street (Goldstein 1938, p. 552; Rouse 1946, p. 241; Rosenhead 1963, opp. p. 105; Batchelor 1967, plate 2; van Dyke 1982, pp. 4–5, 56–57; Perry *et al.* 1982, opp. p. 90; Tritton 1988, pp. 25–26), and the turbulent wake that occurs instead at still higher Reynolds number (van Dyke 1982, p. 31; Tritton 1988, p. 30).

The von Kármán vortex street: a simple model

We now model a fully formed vortex street (Fig. 5.14(*d*, *e*)) by one set of line vortices of strength Γ at $z = na$, and another set of strength $-\Gamma$ at $z = (n + \frac{1}{2})a + ib$, with $n = 0, \pm 1, \pm 2 \ldots$ (see Fig. 5.15). As in §5.6 we assume that each line vortex moves at the local flow velocity due to everything other than itself, this being a crude substitute for having finite patches of vorticity which move according to eqn (5.9).

Consider any vortex. The local flow velocity due to the others in the same row is zero, because their contributions cancel in pairs. The y-components of velocity due to those in the other row also cancel in pairs, but the x-components reinforce each other to give a certain velocity V to the left (if $\Gamma > 0$). This velocity is common to all the vortices, so the whole array moves to the left at this speed, while maintaining its form.

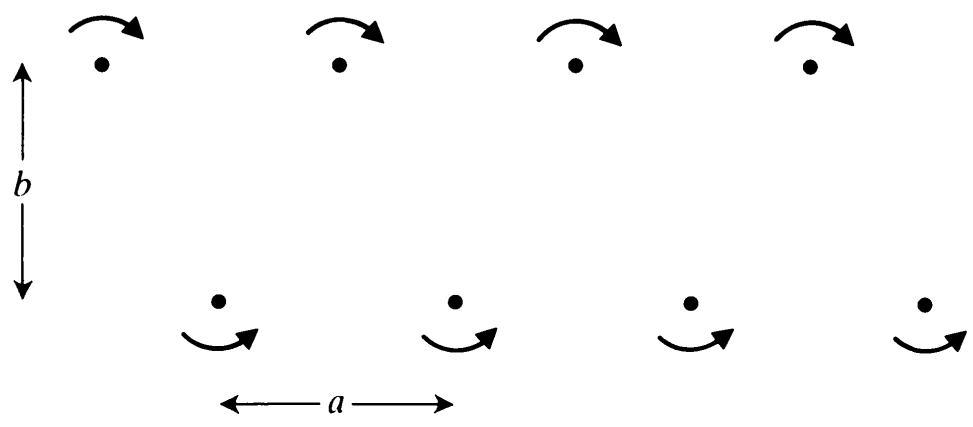

Fig. 5.15. Line vortex representation of a von Kármán vortex street.

To find V, let us calculate $\mathrm{d}w/\mathrm{d}z$ at, say, $z = \frac{1}{2}a + \mathrm{i}b$, where w is the complex potential due to the whole of the bottom row. The complex potential due to the member of that row at $z = na$ may be written as

$$-\frac{\mathrm{i}\Gamma}{2\pi}\log(z - na),$$

but we note, as a preliminary, that an equally good representation of this particular flow is

$$-\frac{\mathrm{i}\Gamma}{2\pi}\log\left(1 - \frac{z}{na}\right), \qquad (n \neq 0),$$

for the two differ only by an additive constant, which makes no difference to the resulting flow. The complex potential due to the whole of the bottom row can therefore be written

$$w = -\frac{\mathrm{i}\Gamma}{2\pi}\sum_{-\infty}^{-1}\log\left(1 - \frac{z}{na}\right) - \frac{\mathrm{i}\Gamma}{2\pi}\log z - \frac{\mathrm{i}\Gamma}{2\pi}\sum_{1}^{\infty}\log\left(1 - \frac{z}{na}\right)$$

$$= -\frac{\mathrm{i}\Gamma}{2\pi}\log\left[z\prod_{n=1}^{\infty}\left(1 - \frac{z^2}{n^2a^2}\right)\right]$$

$$= -\frac{\mathrm{i}\Gamma}{2\pi}\log\left(\sin\frac{\pi z}{a}\right) + \text{constant}, \qquad (5.29)$$

where we have used an identity drawn from complex variable theory (e.g. Carrier *et al.* 1966, p. 97). Thus

$$\frac{\mathrm{d}w}{\mathrm{d}z} = -\frac{\mathrm{i}\Gamma}{2a}\cot\left(\frac{\pi z}{a}\right),$$

whence

$$\left.\frac{\mathrm{d}w}{\mathrm{d}z}\right|_{z=\frac{1}{2}a+\mathrm{i}b} = \frac{\mathrm{i}\Gamma}{2a}\tan\left(\frac{\mathrm{i}\pi b}{a}\right) = -\frac{\Gamma}{2a}\tanh\left(\frac{\pi b}{a}\right).$$

The whole vortex street therefore moves to the left with speed

$$V = \frac{\Gamma}{2a}\tanh\left(\frac{\pi b}{a}\right). \qquad (5.30)$$

This accounts for why the von Kármán vortices in Fig. 5.14(*d*) give chase to the cylinder, and why, relative to the cylinder, they are not swept downstream at quite the free stream speed U.

5.8. Instability of vortex patterns

Von Kármán went on to consider what happens if the vortices in Fig. 5.15 are slightly displaced from their correct positions. He showed that such displacements do not remain small as time proceeds, so that the basic configuration is unstable, except in the case

$$\cosh\frac{\pi b}{a} = \sqrt{2}, \qquad \text{i.e. } b/a \doteqdot 0.281, \tag{5.31}$$

when his analysis revealed no instability. The relevance or otherwise of this special value of b/a to real vortex streets has caused much consternation over the years, the issue being clouded by the subsequent discovery that the system is more weakly unstable even in the case (5.31).

Another classical problem involves the stability of n line vortices spaced regularly around the circumference of a circle of radius a. Now, it is obvious that two vortices of strength Γ, placed a distance $2a$ apart, will rotate about the mid-point of the line joining them with angular velocity $\Gamma/4\pi a^2$, because each induces a velocity $\Gamma/4\pi a$ perpendicular to that line at the position occupied by the other (Fig. 5.16(a)). More generally, it can be shown that n equal line vortices can maintain themselves in a circular array by rotating with angular velocity

$$\Omega = (n-1)\frac{\Gamma}{4\pi a^2}, \tag{5.32}$$

where Γ denotes the circulation around any one such vortex

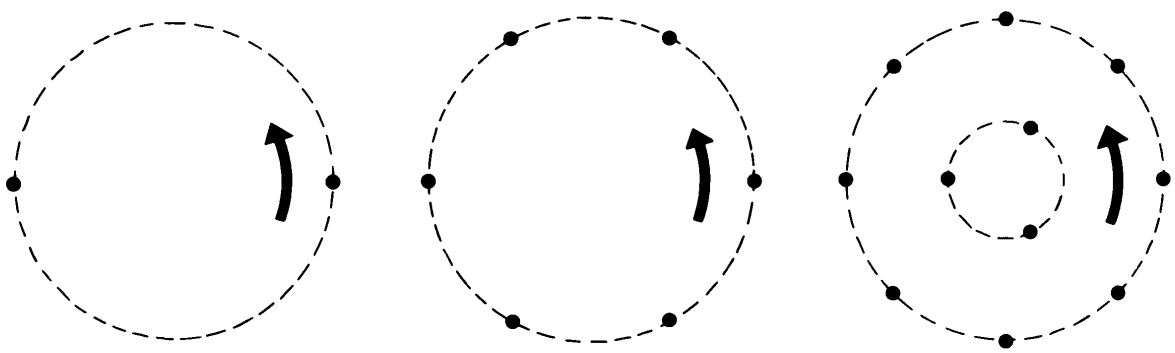

(a) (b) (c)

Fig. 5.16. Stable rotating configurations of 2, 6, and 11 line vortices.

(Exercise 5.14). The stability of this motion was first investigated in 1883 by J. J. Thomson, who later discovered the electron. He concluded that the motion was stable when $n < 7$ and unstable when $n \geqslant 7$, but the case $n = 7$ was subsequently shown to be neutrally stable by Havelock in 1931. It is chastening to find this apparently academic problem having very real application, nigh on a century after Thomson's analysis, to superfluid hydrodynamics.† In liquid helium, at temperatures extremely close to absolute zero, unusual line vortices are observed, each with a circulation Γ which is quantized and equal to $\hbar/m$, where $\hbar$ is Planck's constant and m is the mass of the ^{4}He II atom. These vortices can be observed rotating in various types of array (e.g. Fig. 5.16(*c*)), but, notably, only in the singly circular arrays of Fig. 5.16(*a*, *b*) if $n < 7$, as the stability results would suggest (see the photograph in Yarmchuk *et al.* (1979) and Table II of Campbell and Ziff (1979)).

We turn now to the evolution of finite patches of concentrated vorticity. An early example was provided by Kirchhoff in 1876, who showed that an elliptical patch of uniform vorticity ω will rotate with angular velocity

$$\Omega = \frac{ab}{(a+b)^2}\,\omega, \tag{5.33}$$

where a and b denote the semi-axes of the elliptical region (see Lamb 1932, p. 232). Some years later, in 1893, Love showed that this simple motion is unstable if b/a is greater than 3 or less than $\frac{1}{3}$, and the subsequent evolution of such a vortex has been investigated by Dritschel 1986 (see especially his Figs 12–14).

A circular array of n finite patches of vorticity—a sort of smeared-out version of Fig. 5.16(*a*, *b*)—turns out to be unstable even when $n < 7$, if the patches are big enough, the critical size being larger for smaller values of n (Dritschel 1985, see especially his Fig. 2 and §7).

We remarked above that the classical von Kármán vortex street is stable for just one spacing ratio $b/a = 0.281$, at least according to linear theory (exemplified by Exercise 5.13). If the

† This field seems to provide a wealth of other exotic applications of classical, strictly inviscid, flow theory (see Roberts and Donnelly 1974, especially pp. 184–186, 196–199, 210–211; also Donnelly 1988).

vortices have small but finite cross-sectional area A, there remains just one spacing ratio for which the street is stable on linear theory, this ratio being close to the von Kármán value and only weakly dependent on the small parameter A/a^2 (Meiron *et al.* 1984). This hard-earned result was somewhat unexpected (but see the survey of the whole problem in the introduction to Jimenez (1987)).

The evolution of a continuous 2-D distribution of vorticity

$$\omega = \frac{\partial v}{\partial x} - \frac{\partial u}{\partial y}$$

is of course governed by the vorticity equation (5.9)

$$\frac{\partial \omega}{\partial t} + u\frac{\partial \omega}{\partial x} + v\frac{\partial \omega}{\partial y} = 0, \tag{5.34}$$

together with

$$\frac{\partial u}{\partial x} + \frac{\partial v}{\partial y} = 0. \tag{5.35}$$

Now, eqn (5.34) implies that ω is conserved for an individual fluid element, and the incompressibility condition (5.35) implies that the element's cross-sectional area in the x–y plane is conserved, so

$$\int \omega \, \mathrm{d}S = \text{constant}, \tag{5.36}$$

the integral being taken over the whole plane of the flow. There are other relationships of this kind:

$$\int x\omega \, \mathrm{d}S = \text{constant}, \qquad \int y\omega \, \mathrm{d}S = \text{constant} \tag{5.37}$$

(see Batchelor (1967, p. 528), and see Exercise 5.15 for the equivalent result for line vortices), and such conserved quantities provide valuable constraints on how distributions of vorticity can evolve.

A particularly interesting case is that of *vortex merging*. Suppose that, at $t = 0$, two circular patches of uniform and equal vorticity, each of radius R, have centres a distance d apart. Then if d/R is greater than about 3.5 the (deformed) patches end up

rotating about a common centre, much as do two line vortices of equal strength (Fig. 5.16(*a*)). But if d/R is less than 3.5 the vortex patches quickly merge, and to satisfy the conservation laws they do this by wrapping around each other with irrotationally moving fluid entrained between them like the jam in a Swiss roll (Aref (1983), and see also the outstanding photographs of a computer simulation of this process by Seren *et al.*, in Reed (1987)).

While two nearby like-signed vortices tend to merge in this way, two nearby patches of vorticity of opposite sign stand a chance of escaping from the vicinity of other such patches, essentially as a lone vortex pair. An interesting example of this occurs in the work of Cattaneo and Hughes (1988; see especially their Figs 6 and 8). This behaviour has also been observed in the truly remarkable soap-film experiments of Couder and Basdevant (1986). By towing a cylinder through a soap film they produce some extraordinary phenomena which are, presumably, lurking in the 2-D equations of motion, but which are usually obscured in more conventional experiments by an assortment of 3-D instabilities (see especially their Figs 3 and 7).

5.9. A steady viscous vortex maintained by a secondary flow

The Helmholtz vortex theorems are about the convection of vortex lines with the fluid and the intensification of vorticity when vortex lines are stretched. In a viscous fluid there is also diffusion of vorticity (see §§2.3–2.5), and the three processes correspond, respectively, to the second, third, and fourth terms in the vorticity equation (2.39):

$$\frac{\partial \boldsymbol{\omega}}{\partial t} + (\boldsymbol{u} \cdot \nabla)\boldsymbol{\omega} = (\boldsymbol{\omega} \cdot \nabla)\boldsymbol{u} + \nu \nabla^2 \boldsymbol{\omega}. \tag{5.38}$$

There is one exact solution of the Navier–Stokes equations—known as the *Burgers vortex*—which involves all three processes. It is essentially the vortex of Fig. 2.12, but with the radially outward diffusion of vorticity countered by a secondary flow (Fig. 5.17) which (i) sweeps the vorticity back towards the axis and (ii) intensifies the vorticity by stretching fluid elements in the z-direction. The result is a steady, rather than decaying, vortex

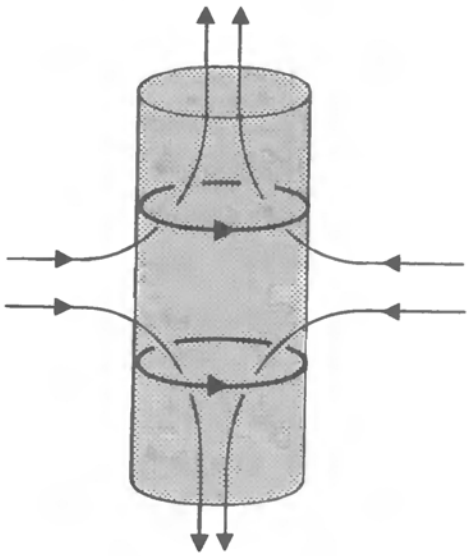

Fig. 5.17. The Burgers vortex.

of the form

$$u_r = -\tfrac{1}{2}\alpha r, \qquad u_z = \alpha z, \qquad u_\theta = \frac{\Gamma}{2\pi r}(1 - \mathrm{e}^{-\alpha r^2/4\nu}) \quad (5.39)$$

(Exercise 5.19), where $\alpha > 0$ and Γ are constants. The velocity profile is sketched in Fig. 5.18.

The vorticity

$$\boldsymbol{\omega} = \frac{\alpha\Gamma}{4\pi\nu}\mathrm{e}^{-\alpha r^2/4\nu}\boldsymbol{e}_z \quad (5.40)$$

is concentrated in a vortex core of radius of order $(\nu/\alpha)^{\frac{1}{2}}$, which is smaller for small viscosity fluids and for strong secondary flows, as one would expect.

The Burgers vortex provides an excellent example of a balance between convection, intensification and diffusion of vorticity, and it is easy to show that without diffusion ($\nu = 0$) the secondary flow makes the vortex stronger and stronger as time proceeds (Exercise 5.18).

The Burgers vortex is, unfortunately, untypical of real vortices in one important respect; the radius of the core is firmly linked to the strength of the secondary flow (via α), but the magnitude of the rotary flow is not—Γ and α are both free parameters in eqn (5.39). This is essentially because there are no rigid boundaries. For real vortices the presence of rigid boundaries plays a crucial part by coupling the magnitudes of the rotary and secondary flows (see §8.5.)

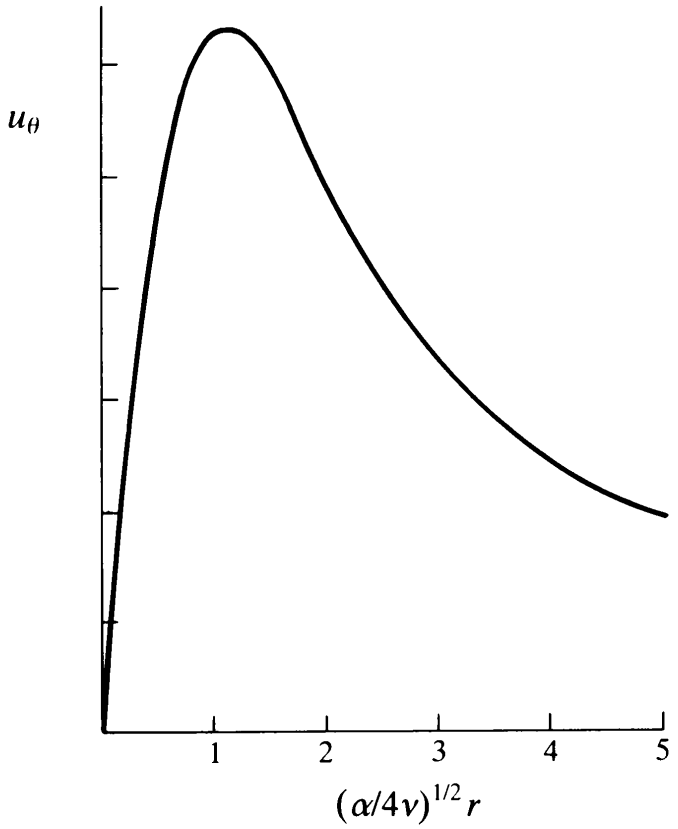

Fig. 5.18. The variation of u_θ with r in a Burgers vortex.

5.10. Viscous vortices: the Prandtl–Batchelor theorem

In the 2-D, steady motion of an inviscid fluid, the equation for the vorticity $\boldsymbol{\omega} = \omega \boldsymbol{k}$ reduces to

$$(\boldsymbol{u} \cdot \nabla)\omega = 0,$$

(see eqn (1.29)), so that ω is constant along any streamline. We may write, then,

$$\boldsymbol{\omega} = [0, 0, \omega(\psi)], \tag{5.41}$$

the stream function ψ being constant along streamlines, as implied by its definition:

$$u = \partial\psi/\partial y, \qquad v = -\partial\psi/\partial x$$

(see eqns (4.5) and (4.7)). The representation (5.41) emphasizes how ω may well be a different constant on different streamlines.

In some cases, as in Fig. 1.8, ω can be determined everywhere without much more ado. In the case of Fig. 1.8, all streamlines can be traced back far upstream, where the vorticity is zero. It follows immediately that the vorticity is zero everywhere.

What happens, however, if there is a region of *closed streamlines* in the flow?

As long as we consider wholly inviscid theory there is in fact nothing we can say about how ω might vary from one streamline to another in such a region. We are, however, as usual, only interested in inviscid theory insofar as it may describe the behaviour of a real fluid *in the limit* $\nu \to 0$, and for the steady flow of a fluid of *non-zero* (but constant) viscosity ν it is the case that

$$\int_C (\nabla \wedge \boldsymbol{\omega}) \cdot \mathrm{d}\boldsymbol{x} = 0, \tag{5.42}$$

where C is any closed streamline (Exercise 5.20).

It is important to note that this integral constraint is exact, and holds for any non-zero ν, however small. Now, in the limit $\nu \to 0$, eqn (5.41) holds and

$$\nabla \wedge (0, 0, \omega) = \left(\frac{\partial \omega}{\partial y}, -\frac{\partial \omega}{\partial x}, 0\right) = \omega'(\psi)\left(\frac{\partial \psi}{\partial y}, -\frac{\partial \psi}{\partial x}, 0\right).$$

Combining this with eqn (5.42) we obtain

$$\omega'(\psi) \int_C \boldsymbol{u} \cdot \mathrm{d}\boldsymbol{x} = 0, \tag{5.43}$$

the function $\omega'(\psi)$ being taken outside the integral because ψ is a constant on the streamline C. The line integral is of course the circulation round the closed streamline C, and will be zero only in exceptional cases; in a typical closed streamline region (such as either of the two eddies in Fig. 5.14(b)) the flow will be in the same sense all round C. So $\omega'(\psi)$ is zero, and this is the Prandtl–Batchelor theorem: in steady, 2-D viscous flow the vorticity is constant throughout any region of closed streamlines *in the limit* $\nu \to 0$.

The computations by Fornberg (1985) of steady flow past a circular cylinder provide a recent example of the theorem at work. These computations give two attached eddies in the wake of the cylinder, so that there are two regions of closed streamlines. Such flows are unstable at high Reynolds number, but they are nevertheless of some interest and importance. In particular, the vorticity in each closed streamline region becomes

progressively more uniform as the Reynolds number R increases, and at $R = 600$ it looks very uniform indeed (see Fornberg's Fig. 9).

Exercises

5.1. Let a closed circuit C of fluid particles be given, at $t = 0$, by

$$\boldsymbol{x} = (a\cos s,\ a\sin s,\ 0), \qquad 0 \leqslant s < 2\pi,$$

so that each value of s between 0 and 2π corresponds to a particular fluid particle. Let $C(t)$ be given subsequently by

$$\boldsymbol{x} = (a\cos s + a\alpha t\sin s,\ a\sin s,\ 0), \quad 0 \leqslant s < 2\pi.$$

Find the velocity $\boldsymbol{u}(s, t)$ of each fluid particle, and show that the particles $s = 0$ and $s = \pi$ remain at rest. Find the acceleration of each fluid particle, show that

$$\boldsymbol{u} = (\alpha y,\ 0,\ 0),$$

and sketch how the shape of $C(t)$ changes with time.

Now, by definition,

$$\Gamma = \int_{C(t)} \boldsymbol{u}\cdot \mathrm{d}\boldsymbol{x} = \int_0^{2\pi} \boldsymbol{u}\cdot\frac{\partial \boldsymbol{x}}{\partial s}\,\mathrm{d}s.$$

Calculate the last integral explicitly at time t, confirming that it is independent of t, in accord with Kelvin's circulation theorem.

5.2. Let $C(t)$ denote a closed circuit composed of the same fluid particles as time proceeds. Then

$$\frac{\mathrm{d}}{\mathrm{d}t}\int_{C(t)} \boldsymbol{u}\cdot \mathrm{d}\boldsymbol{x} = \int_{C(t)} \frac{\mathrm{D}\boldsymbol{u}}{\mathrm{D}t}\cdot \mathrm{d}\boldsymbol{x}. \tag{5.44}$$

To prove this, let $\boldsymbol{x} = \boldsymbol{x}(s, t)$ be a parametric representation of $C(t)$, so that each fluid particle has, throughout the motion, a particular value of s lying between, say, 0 and 1. Then

$$\frac{\mathrm{d}}{\mathrm{d}t}\int_{C(t)} \boldsymbol{u}\cdot \mathrm{d}\boldsymbol{x} = \frac{\mathrm{d}}{\mathrm{d}t}\int_0^1 \boldsymbol{u}\cdot\frac{\partial \boldsymbol{x}}{\partial s}\,\mathrm{d}s = \int_0^1 \frac{\partial}{\partial t}\left(\boldsymbol{u}\cdot\frac{\partial \boldsymbol{x}}{\partial s}\right)\mathrm{d}s,$$

where $\partial/\partial t$ denotes differentiation with respect to *t holding s constant*, s being the variable of integration and the limits on s being fixed. Continue the analysis to establish the result, eqn (5.2).

5.3. Let an ideal fluid be in 2-D motion. By virtue of eqn (5.9) the vorticity ω of any fluid element is conserved. The fluid element must

also conserve its volume, and because it is not being stretched in the z-direction its cross-sectional area δS in the x–y plane must therefore be conserved. It follows that the integral

$$\int \omega \, \mathrm{d}S$$

taken over a dyed cross-section S in the x–y plane, must be independent of time. By Stokes's theorem, or by Green's theorem in the plane (A.24), it follows that Γ, the circulation round the dyed circuit which forms the perimeter of S, must also be independent of time.

This is in some respects a nice way of seeing how Kelvin's circulation theorem comes about. It is, however, a wholly 2-D argument, and that theorem is certainly not restricted to 2-D flows. What is the other serious limitation to the above point of view?

5.4. Show that if we relax the assumptions of incompressibility and constant density in §5.1 then

$$\frac{\mathrm{d}\Gamma}{\mathrm{d}t} = \int_{C(t)} -\frac{1}{\rho} \nabla p \cdot \mathrm{d}\boldsymbol{x} = \int_{C(t)} -\frac{1}{\rho} \frac{\partial p}{\partial s} \mathrm{d}s.$$

A *barotropic* fluid is one for which the pressure p is a function only of the density ρ, so that $p = f(\rho)$. Kelvin's circulation theorem holds for such a fluid; apply Stokes's theorem to the first integral above to give one demonstration of this. What unnecessary assumption is involved in this argument? Construct an alternative proof based on the second integral above.

Use Exercise 1.5 to show that the vorticity equation for a *barotropic* fluid is

$$\frac{\mathrm{D}}{\mathrm{D}t}\left(\frac{\boldsymbol{\omega}}{\rho}\right) = \frac{\boldsymbol{\omega}}{\rho} \cdot \nabla \boldsymbol{u}, \tag{5.45}$$

and note that this is just the vorticity equation (5.7), but with $\boldsymbol{\omega}/\rho$ in place of $\boldsymbol{\omega}$.

As Kelvin's circulation theorem holds, eqn (5.6) is independent of time for a barotropic fluid. Modify the thin vortex-tube argument following the proof of (2) in §5.3 to show that for a barotropic fluid it is $\boldsymbol{\omega}/\rho$, rather than $\boldsymbol{\omega}$, that varies in proportion to l, the length of a small section of the tube.

5.5. Prove that the quantity (5.6) is, at any time, the same for all cross-sections of a vortex tube.

5.6. Show that if $\boldsymbol{a}(\boldsymbol{x}, t)$ is any suitably smooth vector field and

$$\mathscr{C}(t) = \int_{C(t)} \boldsymbol{a} \cdot \mathrm{d}\boldsymbol{x},$$

where $C(t)$ is a circuit consisting of the same fluid particles as time proceeds, then

$$\frac{\mathrm{d}\mathscr{C}}{\mathrm{d}t} = \int_{C(t)} \left\{ \frac{\partial \boldsymbol{a}}{\partial t} + (\nabla \wedge \boldsymbol{a}) \wedge \boldsymbol{u} \right\} \cdot \mathrm{d}\boldsymbol{x}.$$

5.7. Use eqn (5.10) to show that the vorticity equation (5.7) reduces, in the case of axisymmetric flow, to eqn (5.12):

$$\frac{\mathrm{D}}{\mathrm{D}t}\left(\frac{\omega}{R}\right) = 0.$$

5.8. Inviscid fluid occupies the region $x \geqslant 0$, $y \geqslant 0$ bounded by two rigid boundaries $x = 0$, $y = 0$. Its motion results wholly from the presence of a line vortex, which itself moves according to the Helmholtz vortex theorems. Show that the path taken by the vortex is

$$\frac{1}{x^2} + \frac{1}{y^2} = \text{constant}.$$

When an aircraft takes off, the two vortices that trail from its wing-tips (§1.7) are observed to move downwards under each other's influence and then to move further apart as they approach the ground. Why is this?

5.9. *A Bernoulli theorem for unsteady irrotational flow.* Use the momentum equation for an ideal fluid in the form (1.14) to show that for an *irrotational* flow:

$$\frac{\partial \phi}{\partial t} + \frac{p}{\rho} + \tfrac{1}{2}\boldsymbol{u}^2 + \chi = F(t),$$

where ϕ is the velocity potential and $F(t)$ is a function of time alone. (Note, too, that $F(t)$ may be taken to be zero if desired, for its presence is equivalent to adding $\int_0^t F(t_1)\,\mathrm{d}t_1$ to the velocity potential ϕ, which is of no consequence, the velocity field being $\boldsymbol{u} = \nabla\phi$.)

5.10. Inviscid fluid occupies the region $x \geqslant 0$, and there is a plane rigid boundary at $x = 0$. A line vortex of strength Γ is at (d, y_0). Explain why the instantaneous complex potential is

$$w = -\frac{\mathrm{i}\Gamma}{2\pi}\log(z - d - \mathrm{i}y_0) + \frac{\mathrm{i}\Gamma}{2\pi}\log(z + d - \mathrm{i}y_0),$$

and why the vortex moves downward, parallel to the boundary, in such a way that

$$\mathrm{d}y_0/\mathrm{d}t = -\Gamma/4\pi d.$$

Consider, for simplicity, the motion when $y_0 = 0$. Show that at that instant

$$v = -\frac{\Gamma d}{\pi(y^2 + d^2)} \quad \text{and} \quad \frac{\partial \phi}{\partial t} = -\frac{\Gamma^2}{4\pi^2(y^2 + d^2)} \qquad \text{on } x = 0,$$

and hence use Exercise 5.9 to calculate the net force

$$\int_{-\infty}^{\infty} p \, dy$$

exerted on the wall $x = 0$.

What would the force on the wall be if the vortex were somehow fixed at $(d, 0)$?

[This raises questions about the forces involved on the fluid in the core of a vortex when it moves in accord with Helmholtz's theorems, and Lamb (1932, p. 222) makes some interesting observations on the matter.]

5.11. Consider a *symmetric* vortex street in which one set of line vortices of strength Γ is at $z = na$ and the other set, of strength $-\Gamma$, is at $z = na + ib$. Show that the whole array may, in principle, maintain its form by moving to the left with speed

$$V = \frac{\Gamma}{2a} \coth\left(\frac{\pi b}{a}\right).$$

[This configuration is, however, unstable according to linear theory for all values of the spacing ratio b/a; there is no exceptional value corresponding to eqn (5.31). It is still not entirely clear whether this is of any significance in connection with the observed asymmetry of real von Kármán vortex streets, particularly as symmetric streets have, it seems, been observed, albeit under somewhat artificial circumstances (see Taneda 1965; Figs 8a and 9).]

5.12. Suppose that there is, in $y \geq 0$, the irrotational flow

$$u = -\alpha x, \qquad v = \alpha y,$$

where α is a positive constant, and let there be a plane rigid boundary at $y = 0$. Suppose, in addition, there are two line vortices, one of strength $-\Gamma$ at $z = z_1(t)$ and the other of strength Γ at $z = z_2(t)$, where $z = x + iy$. Write down the instantaneous complex potential for the whole flow by the method of images and, by letting the vortices move with the fluid

according to Helmholtz's first vortex theorem, show that

$$\frac{d\bar{z}_1}{dt} = -\frac{i\Gamma}{2\pi}\left[\frac{1}{z_1 - z_2} - \frac{1}{z_1 - \bar{z}_2} + \frac{1}{z_1 - \bar{z}_1}\right] - \alpha z_1,$$
$$\frac{d\bar{z}_2}{dt} = \frac{i\Gamma}{2\pi}\left[\frac{1}{z_2 - z_1} - \frac{1}{z_2 - \bar{z}_1} + \frac{1}{z_2 - \bar{z}_2}\right] - \alpha z_2, \tag{5.46}$$

where an overbar denotes the complex conjugate.

Verify that the vortices may remain at rest at

$$z_1 = d(-1 + i), \qquad z_2 = d(1 + i),$$

where $d^2 = \Gamma/8\pi\alpha$ (see Fig. 5.19(*b*)).

[This system, when rotated clockwise through 90°, may be regarded as a simple model for the attached vortices in Fig. 5.14(*a*, *b*).]

5.13. Investigate the stability of the vortex configuration in Fig. 5.19(*b*) as follows. Introduce dimensionless variables

$$z_1' = z_1/d, \qquad z_2' = z_2/d, \qquad t' = 4\alpha t,$$

and rewrite eqn (5.46) accordingly. Then disturb the vortices slightly, so that

$$z_1' = -1 + i + \varepsilon_1(t), \qquad z_2' = 1 + i + \varepsilon_2(t),$$

where $\varepsilon_1(t)$ and $\varepsilon_2(t)$ are complex variables with moduli which are small compared to 1. Expand the right-hand sides of eqn (5.46) binomially for small $|\varepsilon_1|$ and $|\varepsilon_2|$, and retain only terms of first order in small quantities to obtain

$$4\dot{\bar{\varepsilon}}_1 = -i(\varepsilon_2 - \bar{\varepsilon}_1) + \tfrac{1}{2}(\varepsilon_1 - \bar{\varepsilon}_2) - \varepsilon_1,$$
$$4\dot{\bar{\varepsilon}}_2 = i(\varepsilon_1 - \bar{\varepsilon}_2) + \tfrac{1}{2}(\varepsilon_2 - \bar{\varepsilon}_1) - \varepsilon_2,$$

where the dot denotes differentiation with respect to t'.

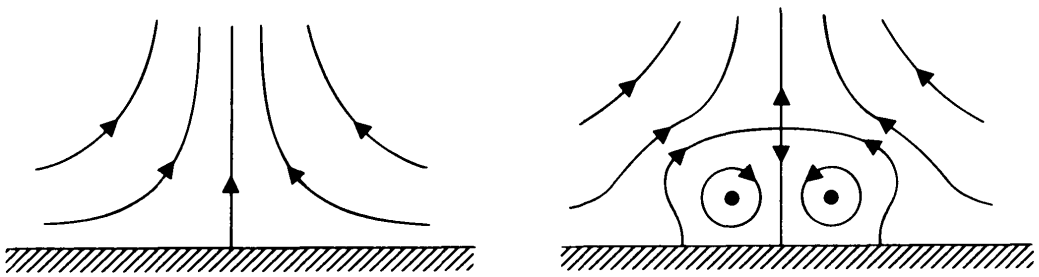

(*a*) (*b*)

Fig. 5.19. Irrotational flow away from a stagnation point (*a*) without and (*b*) with 'attached' vortices.

By introducing suitable new dependent variables in place of ε_1 and ε_2, or otherwise, solve these equations, and thus show that the vortex configuration is unstable, in that any small initial difference in the y-displacements of the two vortices will grow exponentially with time.

[An analysis of this kind with a cylindrical, rather than plane boundary was first carried out by Föppl in 1913, with similar result, and it was the basis for an early theory of how the asymmetry in the downstream positions of the two vortices in Fig. 5.14(c) might come about.]

5.14. Establish that an array of n line vortices of strength Γ, spaced equally around a circle of radius a, can rotate with angular velocity

$$\Omega = (n-1)\frac{\Gamma}{4\pi a^2}.$$

5.15. Let there be line vortices of strength Γ_k at $z = z_k$, where $k = 1, 2, \ldots, n$, each moving under the influence of all the others. Show that if the sth vortex has coordinates (x_s, y_s), then

$$\frac{\mathrm{d}x_s}{\mathrm{d}t} - \mathrm{i}\frac{\mathrm{d}y_s}{\mathrm{d}t} = \frac{-\mathrm{i}}{2\pi}\sum_{\substack{k=1\\k\neq s}}^{n}\frac{\Gamma_k}{z_s - z_k}.$$

Hence show that $\sum_{s=1}^{n}\Gamma_s x_s$ and $\sum_{s=1}^{n}\Gamma_s y_s$ are both constant.

5.16. The *helicity* of a blob of fluid is defined as

$$\int_V \boldsymbol{u}\cdot\boldsymbol{\omega}\,\mathrm{d}V,$$

where the integral is taken over the volume of the blob. Using Reynolds's transport theorem (6.6a) we find that the rate of change of the helicity of a dyed blob of incompressible fluid is

$$\int_V \frac{\mathrm{D}}{\mathrm{D}t}(\boldsymbol{u}\cdot\boldsymbol{\omega})\,\mathrm{d}V.$$

Show that if $\boldsymbol{\omega}\cdot\boldsymbol{n} = 0$ on S, the boundary of V, then the helicity of the blob is conserved.

[The helicity of two closed vortex tubes is crucially dependent on whether or not they are *linked* (Moffatt 1969), and its conservation is then related to the immutability, by virtue of the Helmholtz theorems, of the linkage between such tubes, which led Kelvin to his theory of vortex atoms (see Fig. 5.8).]

5.17. *Ertel's theorem* (1942). Consider the vorticity equation in its form (1.24):

$$\frac{\partial\boldsymbol{\omega}}{\partial t} + \nabla\wedge(\boldsymbol{\omega}\wedge\boldsymbol{u}) = 0.$$

Take the scalar product with $\nabla\lambda$, where $\lambda(\boldsymbol{x}, t)$ is any scalar function of position and time that we care to choose, and then use vector identities to show that

$$\frac{\mathrm{D}}{\mathrm{D}t}(\boldsymbol{\omega}\cdot\nabla\lambda) = (\boldsymbol{\omega}\cdot\nabla)\frac{\mathrm{D}\lambda}{\mathrm{D}t}.$$

Hence deduce that *if $\lambda(\boldsymbol{x}, t)$ is any scalar quantity which is conserved by individual fluid elements, then $\boldsymbol{\omega}\cdot\nabla\lambda$ is likewise conserved.*

[This is actually a special case of the theorem, which is not restricted to incompressible fluids of constant density.]

5.18. *An intensifying vortex.* Consider the flow

$$x = \mathrm{e}^{-\frac{1}{2}\alpha t}\left[X\cos\left\{\frac{\Omega}{\alpha}(\mathrm{e}^{\alpha t}-1)\right\} - Y\sin\left\{\frac{\Omega}{\alpha}(\mathrm{e}^{\alpha t}-1)\right\}\right],$$

$$y = \mathrm{e}^{-\frac{1}{2}\alpha t}\left[Y\cos\left\{\frac{\Omega}{\alpha}(\mathrm{e}^{\alpha t}-1)\right\} + X\sin\left\{\frac{\Omega}{\alpha}(\mathrm{e}^{\alpha t}-1)\right\}\right],$$

$$z = Z\mathrm{e}^{\alpha t},$$

where (x, y, z) denotes the position at time t of the fluid particle that was, at $t=0$, at (X, Y, Z) (see Exercise 1.7). Show that

$$\boldsymbol{u} = (-\tfrac{1}{2}\alpha x - \Omega y\mathrm{e}^{\alpha t},\ -\tfrac{1}{2}\alpha y + \Omega x\mathrm{e}^{\alpha t},\ \alpha z)$$

and

$$\boldsymbol{\omega} = (0, 0, 2\Omega\mathrm{e}^{\alpha t}).$$

Verify that $\nabla\cdot\boldsymbol{u} = 0$. Show too that the inviscid vorticity equation (5.7) is satisfied, and note how it describes the rate of change of the vorticity in terms of the stretching of the vortex lines resulting from the increase of w with z.

Briefly describe the above flow.

5.19. *The Burgers vortex.* Seek an exact, steady solution to the Navier–Stokes equations of the form

$$\boldsymbol{u} = -\tfrac{1}{2}\alpha r\boldsymbol{e}_r + u_\theta(r)\boldsymbol{e}_\theta + \alpha z\boldsymbol{e}_z,$$

where α is a positive constant. Note that $\boldsymbol{\omega} = \omega\boldsymbol{e}_z$, where

$$\omega = \frac{1}{r}\frac{\mathrm{d}}{\mathrm{d}r}(ru_\theta).$$

Verify that $\nabla\cdot\boldsymbol{u} = 0$, and show that the equations of motion imply

$$-\tfrac{1}{2}\alpha r\omega = \nu\frac{\mathrm{d}\omega}{\mathrm{d}r}.$$

Deduce that

$$u_\theta = \frac{\Gamma}{2\pi r}(1 - e^{-\alpha r^2/4\nu}),$$

where Γ is an arbitrary constant.

5.20. *Steady viscous flow with closed streamlines.* The steady momentum equation for an incompressible viscous fluid of constant density ρ is

$$(\boldsymbol{u} \cdot \nabla)\boldsymbol{u} = -\nabla(p/\rho) + \nu\nabla^2\boldsymbol{u}.$$

Rewrite the first and last terms by means of suitable vector identities, and then integrate both sides round a closed streamline C to show that

$$\nu \int_C (\nabla \wedge \boldsymbol{\omega}) \cdot d\boldsymbol{x} = 0,$$

where $\boldsymbol{\omega} = \nabla \wedge \boldsymbol{u}$.

5.21. *Cauchy's vorticity formula* (1815). Let a fluid particle be at position $\boldsymbol{X}$ at $t = 0$, and let the vorticity there be $\boldsymbol{\omega}_0$ at $t = 0$. Let the subsequent motion of the fluid particle be described by $\boldsymbol{x} = \boldsymbol{x}(\boldsymbol{X}, t)$ as, for example, in Exercise 5.18. (This description will have a unique inverse $\boldsymbol{X} = \boldsymbol{X}(\boldsymbol{x}, t)$.) Let the vorticity of the fluid at $\boldsymbol{x}$, the position of the particle at time t, be $\boldsymbol{\omega}$. Then Cauchy proved that $\boldsymbol{\omega}$ is related to $\boldsymbol{\omega}_0$ by

$$\omega_i = \omega_{0j}\frac{\partial x_i}{\partial X_j}, \qquad i = 1, 2, 3,$$

where $\boldsymbol{x} = (x_1, x_2, x_3)$, $\boldsymbol{X} = (X_1, X_2, X_3)$, and summation over $j = 1, 2, 3$ is understood, by virtue of the repeated suffix.

Confirm, first, that this formula holds in the particular case of Exercise 5.18, and then prove that it holds in general.

[One way is to use Ertel's theorem (Exercise 5.17) on three scalar quantities that are rather trivially constant following a particular fluid element; this gives $\boldsymbol{\omega}_0$ in terms of $\boldsymbol{\omega}$, which then has to be inverted.]

5.22. *Alternative proof of the laws of vortex motion.* Let $\boldsymbol{X} = \boldsymbol{X}(s)$ denote a line of dyed particles in the fluid, at $t = 0$, s denoting distance along the line at that time, and suppose that the line is also a vortex line. Use Cauchy's vorticity formula (Exercise 5.21) to show that the dyed particles continue to lie on a vortex line. Investigate, too, the magnitude of the vorticity, $|\boldsymbol{\omega}|$, in the neighbourhood of any particular dyed segment, showing that $|\boldsymbol{\omega}|$ increases with time in proportion to the length of that segment.

Miscellaneous exercises on irrotational flow

5.23. Ideal fluid moves irrotationally in a simply connected region V bounded by a closed surface S, so that $\boldsymbol{u} = \nabla\phi$, where ϕ is the velocity potential. Show that

$$\nabla^2\phi = 0,$$

and that the kinetic energy

$$T = \tfrac{1}{2}\rho \int_V \boldsymbol{u}^2 \, \mathrm{d}V$$

can therefore be written in the form

$$T = \tfrac{1}{2}\rho \int_S \phi \frac{\partial\phi}{\partial n} \, \mathrm{d}S.$$

5.24. *Uniqueness of irrotational flow.* Ideal fluid moves in a bounded simply connected region V, and the normal component of velocity $\boldsymbol{u} \cdot \boldsymbol{n}$ is given (as $f(\boldsymbol{x}, t)$, say) at each point of the boundary of V. Show that there is at most one irrotational flow in V which satisfies the boundary condition.

[This explains why such flows cannot, typically, satisfy a no-slip condition as well. The theorem may, in addition, be extended to encompass unbounded simply connected regions of irrotational flow, as in the case of a sphere moving through a fluid at rest at infinity.]

5.25. *Kelvin's minimum energy theorem.* Consider the various smooth velocity fields $\boldsymbol{u}(\boldsymbol{x}, t)$ in a simply connected region V that satisfy (i) $\nabla \cdot \boldsymbol{u} = 0$ and (ii) the condition $\boldsymbol{u} \cdot \boldsymbol{n} = f(\boldsymbol{x}, t)$ on S, the boundary of V. (We suspend, then, for the present, all consideration of whether or not the velocity fields would be dynamically possible.) Show that the (unique) irrotational flow has less kinetic energy than any of the others.

5.26. In §5.5 the problem of irrotational flow past a rigid sphere was formulated, and solved, in terms of the Stokes stream function Ψ. Re-work the problem in terms of the velocity potential ϕ, which satisfies the axisymmetric version of Laplace's equation (5.4), i.e.

$$\frac{1}{r^2}\frac{\partial}{\partial r}\left(r^2\frac{\partial\phi}{\partial r}\right) + \frac{1}{r^2\sin\theta}\frac{\partial}{\partial\theta}\left(\sin\theta\frac{\partial\phi}{\partial\theta}\right) = 0.$$

Check that the 'slip velocity' on the sphere is eqn (5.22), as before. Show that the pressure distribution on the sphere is symmetric, fore and aft, so that the drag on the sphere is zero.

5.27. A sphere of radius a moves in a straight line with speed $U(t)$ through inviscid incompressible fluid which is at rest at infinity. Explain

why, at the instant the sphere passes the origin,

$$\frac{\partial \phi}{\partial r} = U(t)\cos\theta \qquad \text{on } r = a,$$

where r and θ are spherical polar coordinates, the polar axis ($\theta = 0$) being in the direction in which the sphere is moving. Show that at the instant in question

$$\phi = -\frac{U(t)a^3}{2r^2}\cos\theta.$$

Calculate the kinetic energy of the instantaneous fluid motion, and show, by considering the rate of working of the sphere on the fluid, that the sphere experiences a drag force

$$D = \tfrac{1}{2}M\frac{\mathrm{d}U}{\mathrm{d}t},$$

where M denotes the mass of liquid displaced by the sphere.

5.28. Two plane rigid boundaries $\theta = \pm\Omega t$ are rotating with equal and opposite angular velocities Ω, and there is inviscid fluid in the region between them, $0 < r < \infty$, $-\Omega t < \theta < \Omega t$. The flow is irrotational, so a velocity potential $\phi(r, \theta, t)$ exists which satisfies the 2-D version of eqn (5.4) in cylindrical polar coordinates, i.e.

$$\frac{1}{r}\frac{\partial}{\partial r}\left(r\frac{\partial \phi}{\partial r}\right) + \frac{1}{r^2}\frac{\partial^2 \phi}{\partial \theta^2} = 0.$$

Use the method of separation of variables to find the velocity potential $\phi(r, \theta, t)$, and then use eqn (4.9) to find the stream function $\psi(r, \theta, t)$. Sketch the streamlines at time t. Find the pressure p on the boundaries as a function of r and t.

Show that the whole solution breaks down when the angle between the boundaries increases to π, but that until that time the origin is a stagnation point for the flow.

[This last result is of practical significance in connexion with the 'fling' in Fig. 5.3.]

5.29. Ideal fluid occupies the gap $a < r < b$ between two infinitely long cylinders, which are fixed. The irrotational flow between them is

$$\boldsymbol{u} = \frac{\Gamma}{2\pi r}\boldsymbol{e}_\theta,$$

where Γ is a constant. 'As there is no normal velocity on either bounding surface, $r = a$ or $r = b$, we find from the last result in Exercise 5.23 that the kinetic energy is zero.' This is evidently absurd. Explain the fallacy, and show how to use the last result in Exercise 5.23 correctly to give the kinetic energy of the flow.